AD-A031 228 AUSTRALIAN NATIONAL UNIV CANBERRA RESEARCH SCHOOL OF--ETC F/G 4/2
SOLITARY WAVES IN THE ATMOSPHERE.(U)
AUG 76 D R CHRISTIE, K J MUIRHEAD, A L HALES AF-AFOSR-2759-75

UNCLASSIFIED 76-1 AFOSR-TR-76-1133 NL

1 OF 1
ADA031228

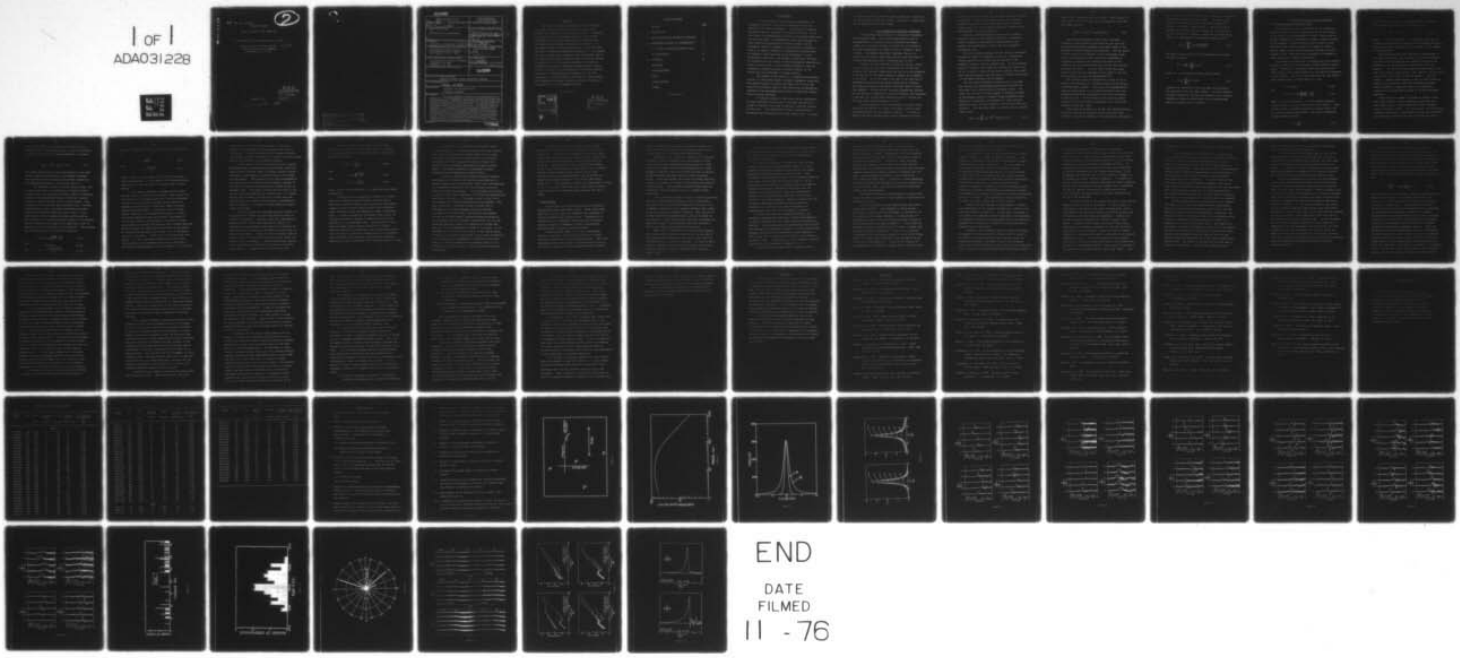

END

DATE
FILMED
11 -76

AFOSR - TR - 76 - 1133

TECHNICAL REPORT

SOLITARY WAVES IN THE ATMOSPHERE

D.R. Christie, K.J. Muirhead, and A.L. Hales

Research School of Earth Sciences,
Australian National University,
Canberra, A.C.T., 2600

1 August 1976

AIR FORCE OFFICE OF SCIENTIFIC RESEARCH (AFSC)
NOTICE OF TRANSMITTAL TO DDC
This technical report has been reviewed and is
approved for publication release IAW AFR 190-12 (7b).
Distribution is unlimited.
A. D. BLOSE
Technical Information Officer

UNCLASSIFIED

REPORT DOCUMENTATION PAGE		READ INSTRUCTIONS BEFORE COMPLETING FORM
1. Report Number AFOSR - TR - 76 - 1133	2. Govt Accession No.	3. Recipient's Catalog Number
4. Title (and Subtitle) SOLITARY WAVES IN THE ATMOSPHERE.		5. Type of Report & Period Covered Interim rept. for Period ending June 30, 1976
		6. Performing Org. Report Number 76 - 1
7. Author(s) Christie, D.R., Muirhead, K.J. & Hales, A.L.		8. Contract or Grant Number AF-AFOSR - 75-2759A
9. Performing Organization Name and Address Research School of Earth Sciences, The Australian National University, Box 4, Canberra A.C.T. 2600		10. Program Element, Project, Task Area & Work Unit Numbers 6799 AF-6799
11. Controlling Office Name and Address Air Force Office of Scientific Research, Bolling Air Force Base, Washington D.C. 20332		12. Report Date 1 August, 1976
		13. Number of Pages 59
14. Monitoring Agency Name and Address		15. UNCLASSIFIED

16. & 17. Distribution Statement

Approved for public release; distribution unlimited.

18. Supplementary Notes

TECH, OTHER

19. Key Words

Atmospheric solitary gravity waves

Atmospheric turbulence

20. Abstract

This report presents a description and interpretation of an unusual type of isolated atmospheric gravity wave observed near Tennant Creek in central Australia. Comparison of experimental data with theory shows that waves of this type belong to a new class of deep fluid internal solitary wave discovered by Benjamin and by Davis and Acrivos. An interesting feature of these solitary waves is that they mark the onset of significant atmospheric turbulence. It is proposed that the following source mechanisms play an important role in the creation of solitary atmospheric waves in the arid interior of Australia: i) the impulsive interaction of an intense thunderstorm downdraft or downdraft generated gravity current with an inversion; ii) the interaction of nocturnal katabatic flow with an existing radiation inversion; and iii) the interaction of stationary gravity lee waves or standing eddies with a developing nocturnal inversion following a reversal in the circulation over an orographic feature.

FORM 1473

UNCLASSIFIED

409 896

ABSTRACT

This report presents a description and interpretation of an unusual type of isolated atmospheric gravity wave observed near Tennant Creek in central Australia. Comparison of experimental data with theory shows that waves of this type belong to a new class of deep fluid internal solitary wave discovered by Benjamin and by Davis and Acrivos. An interesting feature of these solitary waves is that they mark the onset of significant atmospheric turbulence. It is proposed that the following source mechanisms play an important role in the creation of solitary atmospheric waves in the arid interior of Australia :(i) the impulsive interaction of an intense thunderstorm downdraft or downdraft generated gravity current with an inversion; (ii) the interaction of nocturnal katabatic flow with an existing radiation inversion; and (iii) the interaction of stationary gravity lee waves or standing eddies with a developing nocturnal inversion following a reversal in the circulation over an orographic feature.

TABLE OF CONTENTS

1. INTRODUCTION

It is well known that the creation, propagation and dissipation of gravity waves play an important role in the dynamics of the earth's atmosphere. The reasons for studying long-period waves of this type are therefore two-fold: in the first place, an understanding of the initial disturbance which gives rise to these waves, the mechanisms by which they propagate and their dispersion characteristics provides insight into the fundamental nature of atmospheric fluid mechanics; secondly, it seems to be equally important to understand the influence that the passage of these waves has on the development of local meterological conditions - for example, gravity waves may often be correlated with the release of latent atmospheric instabilities which in turn give rise to such diverse phenomena as clear air turbulence, propagating squall lines and, possibly, in the extreme case the development of tornado activity.

The purpose of this report is to summarize the principal results of a preliminary study of subsonic atmospheric waves which were observed during the period from August 1975 to June 1976 using a five-component array of high sensitivity microbarometers installed at the Warramunga Seismic Station located near Tennant Creek in central Australia.

Of foremost interest to this study are the observations of large amplitude isolated waves of permanent form which are thought to represent a new type of naturally occurring internal solitary wave. This report will be mainly concerned with a description and interpretation of these unusual waves. A variety

of large amplitude long period dispersed gravity wave trains have also been observed during this period. Discussion of these events will be deferred until a later report.

2. DATA RECORDING AND PROCESSING TECHNIQUES

The Warramunga Seismic Station is situated 37 kilometers SSE of Tennant Creek. The centered quadrilateral array of microbarometers is located on slowly undulating semi-desert terrain at an elevation of about 410 meters MSL with relief in the area encompassed by the array rising to a maximum of about 6 meters. The nearest significant landscape feature is a barren 50 meter granite ridge which runs for about 200 meters in a north-south direction about 1 kilometer east of site 1.

Probably the most important topological features, insofar as the location of this array is concerned, are the 600 meter Murchison and Davenport Ranges which run from 20 to 160 kilometers to the SSE and the 1600 meter Macdonnell Ranges, 450 kilometers to the south. All of the land to the west of the array can be described as semi-featureless stoney desert and an extensive dry steppe area known as the Barkly Tablelands forms the north-east quadrant. Further afield, the major orographical features are the 5000 meter mountains of central New Guinea, 1800 kilometers to the NNE, and the 2400 meter Australian Alps of Victoria and New South Wales, 2300 kilometers to the SE.

The configuration of the five-component infrasonic array along with the location of a vault containing a vertical long-period seismometer are illustrated in Figure 1. An array of Daniels type noise reducing space filters arranged in the form

of a cross with the inlet port at the center has been installed at each site. These filters provide useful suppression of incoherent wind noise in the period range below 20 seconds. A least-squares fit to the measured amplitude response of the microbarometers is shown in Figure 2.

Recently, a SIAP 2000 weather station which provides a continuous record of wind speed and direction, temperature, relative humidity and precipitation was installed midway between the microbarometer at site 1 and the long-period seismometer vault.

The five infrasonic channels and the vertical long-period seismometer channel are sampled at a rate of 2 samples per second, digitized via a 14-bit ADC and recorded in IBM compatible format on 7-track, 556 bpi tape. At the Australian National University these tapes are converted to 9-track, 800 bpi in a compact, 2 data word per 24-bit computer word, format which conserves magnetic tape and which is suitable for analysis on a 48K Harris Datacraft 6024/4 computer.

The main signal processing technique used on the array data consists of a beam-forming program which utilizes the non-linear N-root method devised by Muirhead (1968). The output $e_i(t)$ of the i-th array element is digitally filtered in the bandpass region of interest, properly phased by time shifting to correspond to the passage of a plane wavefront across the array, and then reduced to the N-th root with sign preserved. The resulting product is summed over the n-element array to give

$$R_N(t) = \frac{1}{n} \sum_{i=1}^{n} |\bar{e}_i(t)|^{\frac{1}{N}} \cdot \text{signum}\,(\bar{e}_i(t)) \qquad (2.1)$$

where $\bar{e}_i(t)$ represents the filter output. This quantity is then raised to the N-th power with sign preserved to provide the signal statistic

$$S_N(t) = |R_N(t)|^N \cdot \text{signum}\,(R_N(t)) \qquad (2.2)$$

The principal advantage of this type of automatic infrasonic array processing arises from the fact that this non-linear beam-forming technique gives added weight to the presence of coherent energy in the spectrum. This has proven to be of value in the treatment of data from Tennant Creek due to the prevalence in this semi-desert environment of incoherent, essentially non-Gaussian noise such as that caused by very small whirl-winds (dust devils) which interact with only one sensor. It can be easily shown that large events of this type are suppressed in the output of the N-th root process by a factor of approximately n^{-N}.

All infrasonic data is processed for a value of N=2 in order to take advantage of a hardware square root SAU feature of the Datacraft computer. This output is supplemented by a parallel determination of an integrated polarity stack over the phased array which corresponds to the N-th root process in the limit $N \to \infty$. Further details on the N-th root multi-channel filter may be found in Kanasewich et al. (1973) and Muirhead and Ram Datt (1976).

Power spectral estimates of the data are computed directly using the Fast Fourier Transform (Cooley and Tukey, 1965). In order to reduce the variance of the estimate the calculations

are carried out using the method of time averaging over modified periodograms described by Welch (1967). The digital time series t_r is divided into K portions each of length $M=2^{10}$ points; the elements in each segment i are then weighted according to a cosine taper data window d_r effective over the 10% limits of the segment, as suggested by Bingham et al. (1967), and transformed to the frequency domain to give

$$X_i(f) = \sum_{r=0}^{M-1} d_r t_r \exp\left\{\frac{-2\pi irf}{M}\right\} \qquad (2.3)$$

The power spectral density is then determined by averaging over the K segments,

$$\overline{P}(f) = \frac{2\Delta t}{KMU} \sum_{i=1}^{K} |X_i(f)|^2, \qquad (2.4)$$

where Δt is the sampling interval and the factor

$$U = \frac{1}{M} \sum_{r=1}^{M} d_r^2 = 0.875 \qquad (2.5)$$

preserves the invariance of the area under the spectrum to the influence of the data taper window. The power spectral estimates obtained in this way are converted to true spectral estimates by dividing by the square of the microbarograph amplitude response shown in Figure 2.

3. EXPERIMENTAL RESULTS AND INTERPRETATION

3.1 Internal Solitary Atmospheric Waves

The phenomenon of the solitary wave, by its essentially nonlinear nature, occupies a unique place in the development of the theory of wave propagation in fluids. These waves are usually defined (Lamb, 1932, §252) as waves of single elevation which propagate at uniform velocity without change of form. They arise from a balance between the tendency of waves to steepen ahead of their crests (amplitude dispersion) and the tendency of the longer period wave components to propagate at higher velocities (frequency dispersion).

The classical solitary wave of elevation was first observed by Russell (1844) on the free surface of shallow water of uniform depth. Subsequently, Boussinesq (1871) and Rayleigh (1876) independently derived approximations for the speed of propagation, c, and the form, $\eta(x)$, of the wave profile at the free surface. These authors found, to first order in $\alpha = a/h$,

$$c^2 = gh(1+\alpha) \tag{3.1a}$$

and

$$\eta(x) = a\,\mathrm{sech}^2\left\{\left(\frac{3a}{h+a}\right)^{\frac{1}{2}}\frac{x}{2h}\right\}, \tag{3.1b}$$

where h is the fluid depth, a is the maximum amplitude of the wave and g is the acceleration due to gravity. These results reveal an important property of solitary waves; that is, they are always supercritical - the speed of propagation walways exceeds the speed

$$c_o = \sqrt{gh} \tag{3.2}$$

of infinitesimal long waves. This property may be expressed to first order in the dimensionless amplitude as

$$F^2 = 1 + \alpha > 1 \qquad (3.3)$$

where F is the Froude number. It should be noted that the classical solitary wave is derived on the simplifying assumption that the horizontal length scale of the motion is long compared to the fluid depth.

Korteweg and DeVries (1895) were able to demonstrate, in the first approximation, the existence of a class of periodic long waves of finite amplitude and permanent form which are described by the Jacobi elliptic function $aCn^2(x/\lambda,k)$ of modulus k. In particular, they showed that these waves, which they called *cnoidal* waves, reduce to the classical solitary wave of finite extent in the limit as the wavelength, λ , goes to infinity. Despite this progress, it was not until relatively recently that Lavrentiev (1946) and Friedrichs and Hyers (1954) succeeded in rigorously proving the mathematical existence of a solitary wave solution of the full non-linear equations.

There have been a number of attempts to improve on the first order solution for the classical solitary wave (e.g., Long (1956b);Laitone (1960); Byatt-Smith (1970); Grimshaw (1971); and Fenton (1972)). The most accurate results are those of Fenton, who obtained a ninth-order solution, and Byatt-Smith who numerically solved for the case of the solitary wave an

exact integro-differential equation for surface waves of permanent form. The principal result of these investigations is that the solitary wave of maximum amplitude corresponds to

$$\alpha_{max} = 0.85 \ , \ F_{max} = 1.31 \ . \qquad (3.4)$$

It is worth noting that the first approximation to the shape of the classical solitary wave (3.1b) compares favourably with the exact profile computed by Byatt-Smith provided the non-dimensional amplitude α is less than about 0.7.

The theoretical study of internal solitary waves, that is, waves which exist as a consequence of internal density stratification, was initiated by Keulegan (1953) who considered a system of two superimposed liquids of different constant densities, bounded above and below by rigid surfaces. Long (1956b) has also investigated this particular model. Abdullah (1956) obtained, using a systematic perturbation procedure developed by Friedrichs (1948) and Keller (1948), a first order solution for the classical internal solitary wave at the interface of a two-layer atmosphere subject to the condition that the hydrostatic law holds for the upper layer, that is, that motion of the free surface can be neglected. This solution is a supercritical wave of elevation described by

$$\eta(x) = a \ \mathrm{sech}^2\left\{\sqrt{\frac{3\alpha}{2}} \ \frac{x}{h}\right\} \qquad (3.5a)$$

and

$$c = c_o'(1+\tfrac{1}{2}\alpha) \qquad (3.5b)$$

with

$$w_{\frac{1}{2}} = \frac{4 \log_e(1+\sqrt{2})}{3\alpha} \, h \qquad (3.5c)$$

where the infinitesimal internal wave critical speed is given by

$$c_o' = \sqrt{g'h} \tag{3.6}$$

with

$$g' = \frac{g(\rho_1-\rho_2)}{\rho_1} . \tag{3.7}$$

Here, ρ_2 and ρ_1 are the densities of the upper and lower fluids respectively, h is the depth of the undisturbed lower layer and $w_{\frac{1}{2}}$ is the full width of the wave profile at half maximum.

A more general treatment of internal solitary waves has been given by Peters and Stoker (1960). They examined the full problem of a two-fluid system with a free upper boundary as well as the more difficult problem of the existence of internal solitary waves in a fluid whose density decreases exponentially with height. In the case of the two fluid problem they found two solitary-wave solutions; one type, with maximum amplitude at the free surface, corresponds to the ordinary classical solitary wave of elevation; the other type describes an internal solitary wave with a maximum amplitude at the interface much larger than the amplitude at the surface. The internal solitary wave may be either a wave of depression or a wave of elevation. If the depth of the undisturbed lower fluid, h, is less than half the depth of the upper fluid, the streamlines of the disturbance are lines of elevation at the interface and depression at the free surface; if, in addition

the difference in the two fluid densities is small, the solution then corresponds to the approximate form given by (3.5) above. This approximation will be assumed to provide a sufficiently accurate description of classical internal solitary waves in the atmosphere for the present purposes.

In the case of a fluid of finite depth with a density distribution which decreases exponentially upwards, Peters and Stoker found an infinite number of possible internal solitary wave modes corresponding to an infinite spectrum of internal critical speeds. This problem has also been investigated by Long (1965) and, in an elegant and very general treatment of the subject of internal solitary waves in shallow fluids, by Benjamin (1966). The general solitary wave solutions in this case are complicated and will not be given here; it is noted, however, that according to Benjamin the solitary wave mode corresponding to the highest critical speed - predominantly a wave of depression - is probably the most significant mode in fluids of this type.

Up to this point this discussion has been limited to a consideration of internal solitary waves which can exist in fluids of finite depth. Benjamin (1967) and, independently, Davis and Acrivos (1967) have presented the results of a theoretical and experimental investigation of an entirely new class of internal solitary wave phenomenon which can exist in fluids of great depth. These new types of internal waves are shown to exist in regions where the fluid density varies only within a layer of thickness h which is much smaller than the total fluid depth and smaller than the effective horizontal length scale, λ, characteristic of the solitary wave.

For a two fluid system in which the upper fluid extends to infinity over a lower fluid of depth h resting an a horizontal rigid surface, Benjamin finds a solitary wave solution of the form

$$\eta(x) = \frac{a\lambda^2}{x^2+\lambda^2} \tag{3.8a}$$

with

$$c = c_o' \sqrt{1+ \frac{3}{4}\alpha} \tag{3.8b}$$

where

$$2\lambda = w_{\frac{1}{2}} = \frac{8}{3} \frac{\rho_1}{\rho_2} \frac{h}{\alpha} \tag{3.8c}$$

and ρ_2 and ρ_2 are the densities of the upper and lower fluids respectively.

Benjamin has also considered the problem of a shallow fluid with exponential density gradient in contact with a deep fluid of constant density, and, further, the more general problem of solitary waves associated with a thin transition region contained between two homogeneous fluids of substantial depth. In direct analogy with the shallow fluid theory, the continuous variation in density is shown to give rise to an infinite set of solitary-wave modes. For the case of a thin region of sudden vertical density variation in a stably stratified system, the lowest-order mode solitary wave solution takes the form of a bulge which propagates along the interface. This interesting result has been confirmed in the laboratory experiments of Davis and Acrivos (1967) and Hurdis and Pao (1975).

Consider now the existence of solitary-wave motions in the atmosphere. It would seem that the deep fluid solitary wave solution (3.8) found by Benjamin (1967) is best suited to a simple description of solitary waves in the planetary boundary layer while classical solitary wave theory (3.5) should provide a reasonable description of higher altitude waves. The possible existence of atmospheric internal solitary waves was suggested by Abdullah (1949).

In order to clarify the following discussion consider the properties of internal solitary waves associated with a density discontinuity at the 950 mbar (560m) level corrresponding to a temperature inversion of $5^{o}K$, as predicted by both the shallow and deep fluid theories. The air beneath the inversion is taken to have a mean temperature of $270^{o}K$ and the dimensionless amplitude of the wave, α , is chosen to have a value of 0.5, corresponding to a wave with amplitude less than maximum. With these conditions, a classical internal solitary wave as described by (3.5) would propagate along the inversion at a speed of 12.6 m/sec with a full width at half maximum of 1.61 km and would produce a maximum pressure perturbation, ΔP, at ground level of 0.615 mbar; alternatively, for the same amplitude, Benjamin's theory (3.8) describes a solitary wave with $w_{\frac{1}{2}}$ = 3.03 km propagating at a speed of 11.8 m/sec. At the 980 mbar level (280 m), for an inversion of the same intensity, a similar solitary wave would produce a ground level perturbation of 0.317 mbar and would propagate at a velocity of 8.91 m/sec with $w_{\frac{1}{2}}$ = 0.806 km according to the classical theory, or at a velocity of 8.36 m/sec with $w_{\frac{1}{2}}$ = 1.52 km as given by the deep fluid theory.

A comparison of the shallow and deep fluid solitary wave profiles for an inversion at the 950 mbar level is shown in Figure 3. Note that, as a consequence of the short range exponential rise and decay, the influence of the classical wave is much more localized than that of the deep fluid wave of elevation. The shape of both types of solitary wave depends on the value of the dimensionless amplitude α ; as α increases the wave profile narrows and the curvature at the crest increases until at maximum amplitude the wave is reduced to a sharp peak enclosing an angle of 120° (Stokes, 1880; Byatt-Smith, 1970). This variation in profile is illustrated for values of α up to 0.7 by the two families of curves shown in Figure 4 with the depth of the undisturbed fluid taken as the unit of length.

3.2 Observations

A large number of isolated waves have been observed at the infrasonic array near Tennant Creek. These unique waves, which only occur at night, are reasonably well described by the solitary-wave theory outlined above. Consequently, as mentioned in the introduction, these waves are interpreted as being examples of atmospheric internal solitary waves which propagate along the noctural inversion.

Gossard and Munk (1954), in a study of atmospheric pressure oscillations, noted several examples of a gravity wave train preceeded by a positive pressure pulse. These early measurements suffer from a lack of resolution and as such are not directly comparable with the observations made at Tennant

Creek. Nonetheless, on the basis of available evidence, it seems reasonable to assume that these pressure pulses are of the same type as the isolated waves described here.

McAllister et al. (1969) have reported, in a pioneering atmospheric acoustic sounding study, observations of "weak, front-like" nocturnal disturbances characterized by a sharp spike in the sounder record followed immediately by a rapid buildup of turbulence and, after a period of about 10 minutes, by well-developed sinusoidal motion in slowly separating strata. These observations were carried out during the month of June at Ivy Tanks on the edge of the arid Nullarbor Plain in South Australia. These authors interpreted these spikes as reflections from the turbulent core of a somewhat broader disturbance.

A very interesting series of acoustic sounding experiments carried out again during the month of June at Julia Creek, Queensland have been described by Reynolds and Gething (1970). On several occasions they also observed transient sharp spikes on the interface of the nocturnal inversion. Some, but not all of these spikes were associated with a jump in the height of the inversion. These authors noted that waves associated with these sharp spikes on the inversion level might represent a form of non-linear, large amplitude solitary wave.

There is little doubt that the solitary waves observed at the Tennant Creek infrasonic array are of the same type as those observed 800 kilometers to the east at Julia Creek and 1300 kilometers to the south at Ivy Tanks. It does not appear likely at this point that these waves preserve their identity over these distances; however, this possibility should be borne in mind.

Smart (1966) and Jordan (1972) have reported observations of "exponential pressure pulses" near Denver, Colorado, which are similar in many respects to some of the solitary waves described in this report.

The only other evidence for atmospheric solitary waves appears to be the description by Abdullah (1955) of a large amplitude propagating disturbance which appeared over Kansas during the early daylight hours of June 29, 1951. This disturbance, which produced a ground level pressure perturbation of 3.4 mbar, took the form of an elevated mass of cold air propagating on an inversion at a height of about 2 kilometers. The elevated disturbance appeared to extend over about 150 kilometers and was observed to travel with approximately constant form at speeds between 18 m/sec and 24 m/sec over a distance of about 300 kilometers. Abdullah concluded that this disturbance represented an internal solitary wave and attributed its formation to the impulsive movement of a quasistationary cold front into the layer of inversion.

As can be seen from the following description, the atmospheric solitary waves observed at Tennant Creek appear to be entirely different from the single observation described by Abdullah. These subsonic waves are characterized by an initial slow increase in pressure over a period of several minutes which gradually develops into an exponential increase leading to a fairly sharp crest at which point the pressure falls rapidly to the ambient level. A wide variety of these commonly occurring gravity waves are illustrated in Figures 5 to 10.

In most cases, these waves occur as isolated waves of

elevation as shown in Figures 5 and 6. They are usually asymmetrical but a few examples have been observed which are almost symmetrical in form. Occasionally, the initial positive pressure pulse is followed by a wave of depression as shown by the example in Figure 7(a). A number of events have been observed (see Figures 7 to 9) in which the initial positive pressure pulse is followed by several long period large amplitude components which may be either coherent or incoherent over the array - these waveforms are similar to those observed by Smart (1966) and Jordan (1972). Since all of these atmospheric pressure oscillations are initiated by a positive pressure pulse of the same form, these events are all believed to be manifestations of the same phenomena.

The salient features of these atmospheric solitary waves may be seen from an examination of the summary of characteristics presented in Table I.

Waves of this type have been observed with amplitude as high as 700 dynes/cm^2. They propagate at speeds between 4 and 16 m/sec, with an effective wavelength, as measured by the full width at half maximum, between 0.14 kilometers and 2.68 kilometers and tend to occur on successive nights in groups of up to 6 days duration as shown in Figure 11. Even though the available data spans a period of only 10 months, it seems clear that the frequency of occurrence of these waves is seasonal. In contrast to the observations reported by Smart and by Jordan, they do not occur during the daylight hours between 08.30 and 17.00 C.S.T. (see Figure 12). A plot of the frequency of of observation as a function of azimuth (Figure 13) reveals the

fact that these solitary waves originate in the directions of 20^{o} and 140^{o} as measured from true north.

An interesting feature of these solitary waves is their apparent influence on ambient atmospheric conditions. This feature is illustrated in the diurnal variations of the micro-pressure spectrum shown in Figure 14. The last diagram in this series (c) has been chosen to illustrate a typical 40 hour period during which gravity wave activity was absent. As can be seen, the late evening and early morning hours are characterized by a relatively low-level incoherent long-period noise spectrum indicative of a quiet stably stratified noctural atmosphere; in contrast, the onset of daybreak marks a transition to a state of turbulence as the nocturnal inversion is dissipated by the growth of a convectively unstable penetrating layer at the surface. This transition is also accompanied by the onset of a light surface wind of about 4 m/sec.

Consider now the influence of the presence of solitary waves propagating on the nocturnal inversion as is shown in the first two diagrams in Figure 14. In each case, the passage of the isolated wave marks the onset of turbulence in the atmosphere. This remarkable transition is particularly evident following the passage of the second event in Figure 14(b) and may be seen in greater detail in Figure 6(a).

A change in the atmospheric spectral character following the passage of a solitary wave is a feature which is common to all events of this type which have been observed to date in Tennant Creek; however, the degree to which this phenomenon occurs varies over wide limits as can be seen from the comparisons shown in Figure 15 of power spectral densities evaluated before

and after the passage of selected events. The spectra computed from data recorded prior to the passage of the solitary wave are all quite similar and are characteristic of low noise stable conditions as evidenced by the presence of a 4 to 8 second period peak in the spectrum due to microbarom activity. In examples (a) and (b), the solitary wave marks the introduction of spectral components over the complete period range - it is noteworthy that the power from 10 to 100 seconds in example (a) is increased by nearly 4 orders of magnitude. In examples (c) and (d) additional high frequency components are almost completely absent after the passage of the wave; example (d) is interesting in that the spectral characteristics before and after the event are almost identical except for a small contribution in the 10 to 100 second band.

The problem posed by the asymmetrical form of these isolated pressure pulses will now be considered. At first glance, it would seem, on the basis of the theory reviewed above, that if these pressure distributions represent an internal solitary wave of elevation, then they should be symmetrical. However, all of the theoretical treatments are limited to simple static models. Perhaps the most serious criticism of these models when applied to the earth's atmosphere is that the influence of wind shear across the interface (within the limits of dynamic stability) is neglected; this might be the reason for the observed asymmetrical shape. It is also possible that the turbulent wake and form of these pressure pulses result from isolated waves breaking in the backwards direction - this process is enhanced by the presence of a suitable shearing layer (Long, 1956a). This

explanation does not appear to be likely but it should be borne in mind.

Another explanation of these wave forms is indicated by the experimental observations and numerical calculations of Davis and Acrivos (1967) on solitary waves propagating in a thin layer of fluid contained between two deep fluids comprising a stably stratified system. They found that waves of large amplitude develop closed streamlines characteristic of the circulation in a vortex pair and further, that these waves shed semiperiodic waves behind the main disturbance. It follows directly from an argument based on dynamic symmetry (Benjamin, 1967) that a single vortex occurs within large amplitude solitary waves associated with an inhomogeneous shallow layer of fluid lying beneath a much deeper homogeneous fluid and that this internal circulation could lead to the development of a turbulent wake as is observed.

A final possibility which could account for the observed wave shape is that these large amplitude waves significantly displace the fluid above the inversion level and thus they may effect the release of any latent atmospheric instability. The resulting convective mixing would last for a considerable period of time, as observed, and could be expected to result in a rapid drop in pressure to the ambient level. Some support for this idea is provided by a comparison (Figure 16) of the pressure distribution associated with a wave which initiated only slight changes in the atmospheric spectral character with the more typical distribution associated with a wave with a significantly turbulent wake. The profile of the wave with the quiet wake is clearly more symmetrical. However, this interpretation is

open to criticism since some of the observed isolated waves with quiet wakes are strongly asymmetric.

It is worth noting at this point that the *form* of the leading edge of these solitary waves indicates, as could be expected from the atmospheric scale involved, that these waves are best described by the deep fluid internal solitary wave theory. It seems that a final interpretation of these unique waves which includes an explanation of the asymmetric profile will involve more than one of the effects discussed above.

It must be emphasized at this point that any discussion of the source mechanisms which generate these solitary waves is largely conjectural since the range and lateral extent of these waves are almost totally unknown. Existing evidence, such as the fact that these waves traverse the 4 kilometer infrasonic array without noticeable attentuation as highly coherent planar wavefronts, suggests that these waves originate at distances beyond 30 kilometers. If the observed turbulent wake results from an intrinsic tendency of these waves to shed semiperiodic disturbances behind the main body, or, if these waves are breaking, then they are rapidly losing energy and it must therefore be anticipated that they are of limited range. On the other hand, if the observed turbulence results from the disruption of a conditionally unstable atmosphere, then these waves could have a range of up to about 600 kilometers, the limit set by the speed of the wave and the duration of the nocturnal inversion. It is also conceivable that these waves are created by a different form of propagating disturbance which interacts with the nocturnal inversion.

Smart (1966) and Jordan (1972) associated their measured exponential pressure pulses with thunderstorms. The organized, precipitation initiated and maintained downdraft of cold air in severe mature storms is well documented (Wallington, 1961; Browning and Ludlam, 1962; Spillane and McCarthy, 1969). Smart developed a model to describe these pressure pulses by considering the unstable solution of Brunt's equation of motion (Brunt, 1927) for the vertical displacement (dh) of a parcel of air:

$$\frac{d^2(dh)}{dt^2} + \frac{g}{T}(\beta + \frac{dT}{dh})dh = 0 \qquad (3.9)$$

Brunt noted that if the lapse rate, -dT/dh, is greater than the adiabatic lapse rate, β , no restoring force exists, and consequently a downwards displaced air parcel will continue to accelerate exponentially. Smart adapted this result to explain the observed form of the pressure pulses by noting that the downwards descending parcel is subject to a constant pressure gradient and thus the density of the parcel increases exponentially with the result that (assuming the approximate validity of the hydrostatic law) the ground level pressure contains an exponentially increasing component. Smart also hypothesized that the downwards motion continues to accelerate in smooth laminar flow until a critical velocity is reached at which point the flow becomes turbulent and mixes rapidly with nearby warmer air thus causing rapid oscillations behind the pulse and, eventually, a reduction of the pressure to the ambient level. On the basis of this model, Smart was able to account for 4 out of 10 observations of exponential pressure pulses.

There appear to be a number of difficulties associated with this model, the most serious of which is the fact that this explanation is applicable only to observations recorded directly beneath a thunderstorm downdraft; it must be expected that the ground level pressure distribution outside this very localized region is of a completely different form. Consequently, the observations reported by Jordan (1972) of pressure pulses coming from thunderstorms at distances of the order of 100 kilometers are not accounted for by this model as it stands.

It is an obvious extension of this model to include the influence of the shallow gravity current of undercutting cold air that advances away from the thunderstorm as the downdraft spreads out at the surface. Wallington (1961) noted an example in which this density current extended for over 50 kilometers and the subject has recently been treated in detail by Charba (1974). An interesting description of a Sudanese *haboob*, a downdraft gravity current made visible by its high dust content, has been given by Lawson (1971). It is noted that the pressure distribution associated with the passage of a gravity current takes the form of a large change in the pressure level and thus this effect does not, by itself, account for the observed pressure pulse. A more likely explanation of long-range thunderstorm-generated pressure pulses is that they occur as solitary waves produced by either the direct impulsive interaction of the downdraft on an inversion or the concommitant interaction of the gravity current with an existing inversion.

It is possible that some of the solitary waves observed in Tennant Creek during the monsoon season from November to

March are due to thunderstorm activity. However, only 32% of all events that have been observed occurred during periods of local storm activity. A further complication arises from the observation that intense local storms do not necessarily generate solitary atmospheric waves. For example, consider the results of observations made during the month of January, a month characterized by the maximum rainfall, 115.4 mm over a 10 day interval, and the highest number of counts (1490) on a lightning flash counter, as measured at the Warramunga Seismic Station. During this period only one very weak solitary wave was recorded and this particular event occurred on a day when storm activity was entirely absent throughout the Northern Territory.

It is clearly necessary to explore other possible source mechanisms for the solitary atmospheric waves at Warramunga. The fact that these waves come from the preferred directions of 20° and 140° suggests that they are orographic in origin. However, unless one is willing to accept the hypothesis that these waves originate in the atmospheric circulation associated with high mountains, specifically the high mountains of New Guinea and the Australian Alps (or even the Southern Alps of New Zealand) - an unlikely hypothesis for which there is no direct evidence - then, the fact that the topography, on a more reasonable scale of distance, differs considerably in these two source directions, as is described below, indicates that two additional mechanisms may be involved in the production of solitary atmospheric waves in central Australia.

Consider first the origin of isolated waves which arrive from an aximuth of 140°. These waves are most frequently

detected near midnight but they may also occur at any other time during the night. As one proceeds in the direction of 140° from the infrasonic array the terrain can be described as a more or less flat featureless plain for the first 100 kilometers. The Murchison Range begins to appear 5 kilometers to the south of this path at about 10 kilometers from the array. This chain of low hills, which runs parallel to the 140° direction, continues to rise until a maximum elevation of about 200 meters over the surrounding plain is attained at a distance of about 80 kilometers. Beyond 100 kilometers the level plain slowly gives way to the Davenport Range which intersects the Murchison Range at the same altitude, at about 140 kilometers from the array. Further afield in this direction the terrain descends to an arid plain which continues uninterrupted and finally merges with the Simpson Desert at a distance of about 460 kilometers.

The presence of these nearby ranges suggests that the origin of solitary waves coming from this direction is to be found in the interaction with an existing inversion of katabatic (down-slope) nocturnal flow of surface-cooled air from these hills on to the surrounding plain. The hypothesis of supercritical katabatic drainage which leads to an internal hydraulic jump has been employed with considerable success by Ball (1956) (see also, Ball, 1957; Lied, 1964) to explain the sudden stationary discontinuity found in surface winds in the Antarctic. Similarly, Clarke (1972) has explained a frequently occurring, sudden, near-dawn squall on the south coast of the Gulf of Carpentaria by evoking the concept of a propagating undular hydraulic jump created in the process of nocturnal surface flow down a 1:1000 slope from the 500 meter highlands to the

east. Clarke carried out a number of numerical experiments and concluded that internal atmospheric hydraulic jumps of this type should commonly occur at low latitudes when katabatic flow discharges on to a plain under conditions of a stable radiation inversion.

This conclusion is reinforced by the acoustic soundings at Julian Creek reported by Reynolds and Gething (1970) which revealed, as has already been noted, the occurrence of a jump in the height of the nocturnal inversions. These authors also hypothesized the existence of katabatic flow aided in part by the geotrophic wind and orographic convergence and concluded that the observed jumps in the inversion level could be attributed to either the head of a gravity current propagating as an internal bore or a travelling internal hydraulic jump.

It is worth noting at this point that none of the data collected so far from the infrasonic array indicates the occurrence of either a propagating hydraulic jump or the frontal zone of an advancing atmospheric density current. This is not an unexpected result since the local topography indicates that katabatic currents are unlikely to flow in the direction of the array. It is therefore proposed that the observed solitary waves coming from an azimuth of 140^{o} are generated in the interaction of katabatic flow with the noctural inversion and that they propagate along the inversion to the array. It is premature, without further experimental work, to examine this mechanism in detail but it probably takes one of the following forms:

(a) the direct implusive interaction of an advancing gravity current impinging on a established inversion;

(b) the creation of a hydraulic jump at the point where supercritical down-slope flow encounters the horizontal plane - this hydraulic jump may subsequently propagate upstream as flow conditions vary;

(c) the momentary retardation of an advancing bore upon encountering a topographical obstacle such as a ridge or valley, and

(d) the formation of a stationary hydraulic jump in conjunction with a supercritical-subcritical flow transition in the neighbourhood of a topographical barrier.

The interpretation in terms of katabatic flow at an orographic feature accounts for both the occurrence of waves coming from the direction of 140° and for the scarcity of events originating in the north and south-west quadrants where orographic features suitable for the production of katabatic flow are absent. It is possible that a few events originate at long range in the Macdonnell Ranges to the south and south-west.

An attempt to apply an interactive katabatic wind interpretation to account for the source of the large number of solitary events arriving from an azimuth of 20° is less successful. In this direction, the elevation decreases steadily from about 410 meters MSL to 200 meters at a distance of about 150 kilometers from the array. From this point, the land rises slowly to form the Barkly Tablelands at an altitude of about 260 meters. At the edge of the Tablelands, about 340 kilometers from the array, the land again rises to about 310 meters and then falls continuously to the hot tropical coast of the Gulf of Carpentaria, 500 kilometers from the array.

It is possible that solitary waves originating in this direction are produced in the interaction of katabatic flows to the east from either the McDougall Ranges on the outskirts of Tennant Creek or from the Short and Whittington Ranges located a further 50 kilometers to the north. This interpretation is unlikely, however, since these series of ridges rise to a maximum of only 50 meters and the lateral extent of the down-slope run to the surrounding plain would seem to be too limited to support significant katabatic flow. A different type of source mechanism is therefore required to explain the solitary waves which originate in this direction.

An indication of the range of isolated waves coming from an azimuth of 20° is given by the observation that, if one ignores all storm-related signals, all waves of this type arrive at the infrasonic array after 23.30 C.S.T., and further, that the majority of these events are observed to occur around 03.00. This suggests that the source of these waves is to be found at a considerable distance from the array. If it is assumed that these waves are created during or shortly after the formation of a stable inversion then the average measured speed of 10 meters/second is consistent with a source in the neighbourhood of the coastal edge of the Barkly Tablelands.

It is therefore tentatively proposed that these solitary waves are generated through the interaction of a warm upslope sea breeze circulation from the Gulf of Carpentaria with a developing cold nocturnal inversion behind the rim of the Tablelands. This interaction, if not direct, might take the form of an impulsive addition of momentum to the inversion layer

during the collapse of stationary orographic lee waves or during the dissipation of standing eddies following the late afternoon transition from off-shore flow to nocturnal katabatic drainage.

This concludes the description and interpretation of atmospheric internal solitary waves which are observed in the arid interior of Australia.

4. CONCLUSION

This report has been mainly concerned with a description of a new type of naturally occurring solitary atmospheric wave. An examination of the properties of a total of 85 waves of this type, observed over a 10 month period, has shown that these solitary waves propagate along the nocturnal inversion, that they arrive at the infrasonic array from two different azimuths, and that they play an important role in the production of atmospheric turbulence. It is concluded that the solitary waves observed at Warramunga belong to a new class of internal solitary wave discovered by Benjamin and by Davis and Acrivos.

A number of source mechanism which may lead to the production of solitary waves in central Australia have been proposed. Nonetheless, until the completion of further experimental and theoretical work, these ideas must be viewed as conjecture. It is hoped that an expansion of the Warramunga infrasonic array to an aperature of 100 kilometers will provide the necessary data required to determine the origin of these unusual waves.

REFERENCES

Abdullah, A.J., 1949. Cyclogenesis by a purely mechanical process. J. Meteorology, 6, 86-97.

Abdullah, A.J., 1955. The atmospheric solitary wave. Bull. Amer. Met. Soc., 36, 511-518.

Abdullah, A.J., 1956. A note on the atmospheric solitary wave. J. Meteorology, 13, 381-387.

Ball, F.K., 1956. The theory of strong katabatic winds. Aust. J. Phys., 9, 373-386.

Ball, F.K., 1957. The katabatic winds of Adélie Land and King George V Land. Tellus, 9, 201-208.

Benjamin, T.B., 1966. Internal waves of finite amplitude and permanent form. J. Fluid Mech., 25, 241-270.

Benjamin, T.B., 1967. Internal waves of permanent form in fluids of great depth. J. Fluid Mech., 29, 559-592.

Bingham, C., Godgrey, M.D. and Tukey, J.W., 1967. Modern techniques of power spectrum estimation. Trans. IEEE AU-15, 2, 56-66.

Boussinesq, J., 1871. Théorie de l'intumescence liquide appelée onde solitaire ou de translation se propageant dans un canal rectangulaire. Inst. France, Acad. Sci. C.R., June 19.

Browning, K.A. and Ludlam, F.H., 1962. Airflow in convective storms. Quart. J.R. Met. Soc., 88, 117-135.

Brunt, D., 1927. The period of simple vertical oscillations in the atmosphere. Quart. J.R. Met. Soc., 53, 30-32.

Byatt-Smith, J.G.B., 1970. An exact integral equation for steady surface waves. Proc. Roy. Soc. Lond., A.315, 405-418.

Charba, J., 1974. Application of gravity current model to analysis of squall-line gust front. Mon. Wea. Rev., 102, 140-155.

Clarke, R.H., 1972. The morning glory : an atmospheric hydraulic jump. J. Appl. Met., 11, 304-311.

Cooley, J.W. and Tukey, J.W., 1965. An algorithm for the machine calculation of complex Fourier series. Math. Comp., 19, 297-301.

Davis, E.D. and Acrivos A., 1967. Solitary internal waves in deep water. J. Fluid Mech., 29, 593-607.

Fenton, J., 1972. A ninth-order solution for the solitary wave. J. Fluid Mech., 53, 257-271.

Friedrichs, K.O., 1948. On the derivation of the shallow water theory. Appendix to J.J. Stoker, The formation of breakers and bores, Comm. Pure Appl. Math., 1, 81-87.

Friedrichs, K.O. and Hyers, D.H., 1954. The existence of solitary waves. Comm. Pure Appl. Math., 7, 517-550.

Gossard, E. and Munk, W., 1954. On gravity waves in the atmosphere. J. Meteorology, 11, 259-269.

Grimshaw, R., 1971. The solitary wave in water of variable depth. Part 2, J. Fluid Mech., 46, 611-622.

Hurdis, D.A. and Pao, H. Experimental observation of internal solitary waves in a stratified fluid. Phys. Fluids, 18, 385-386.

Jordan, A.R., 1972. Atmospheric gravity waves from winds and storms. J. Atmos. Sci., 29, 445-456.

Kanasewich, C.D., Hemmings, C.D., and Alpaslan, T., 1973. N-th root stack nonlinear multichannel filter. Geophysics, 38, 327-338.

Keller, J.B., 1948. The solitary wave and periodic waves in shallow water. Comm. Pure Appl. Math., 1, 323-339.

Keulegan, G.H., 1953. Characteristics of internal solitary waves. J. Research Nat. Bur. Standards, 51, 133-140.

Korteweg, D.J. and De Vries, G., 1895. On the change of form of long waves advancing in a rectangular canal and on a new type of long stationary waves. Phil. Mag., 39 (5), 422-443.

Laitone, E.V., 1960. The second approximation to cnoidal and solitary waves. J. Fluid Mech., 9, 430-444.

Lamb, H., 1932. Hydrodynamics, 6th edn., Cambridge University Press.

Lavrentiev, M., 1946. On the theory of long waves. Akad. Nauk Ukrain. RSR. Zbirnik Prac. Inst. Mat., No. 5 and No. 8 (1947), 13.

Lawson, T.J., 1971. Haboob structure at Khartoum. Weather, 26, 105-112.

Lied, N.T., 1964. Stationary hydraulic jumps in a katabatic flow near Davis, Antarctica, 1961. Aust. Met. Mag., 47, 40-51.

Long, R.L., 1956a. Long waves in a two-fluid system. J. Meteorology, 13, 70-74.

Long, R.L., 1956b. Solitary waves in one- and two-fluid systems. Tellus, 8, 460-471.

Long, R.L., 1965. On the Boussinesq approximation and its role in the theory of internal waves. Tellus, 17, 46-52.

McAllister, L.G., Pollard, J.R., Mahoney, A.R. and Shaw, P.J.R., 1969. Acoustic sounding - a new approach to the study of atmospheric structure. Proc. IEEE, 57, 579-587.

Muirhead, K.J., 1968. Eliminating false alarms when detecting seismic events automatically. Nature, 186, 704.

Muirhead, K.J. and Ram Datt, 1976. The Nth root process applied to seismic array data. Accepted for publication, Geophys. J. Roy. Astr. Soc.

Peters, A.S. and Stoker, J.J., 1960. Solitary waves in liquids having non-constant density. Comm. Pure Appl. Math., 13, 115-164.

Rayleigh, Lord, 1876. On waves. Phil. Mag., 1(5), 257-279.

Reynolds, R.M. and Gething, J.T., 1970. Acoustic sounding at Benalla, Victoria and Julia Creek, Queensland. Publ. No. 17, Meteor. Department, University of Melbourne, Project EAR, Reports V-VII.

Russell, S., 1844. Report on Waves. British Association Reports, 311.

Smart, E., 1966. An examination of atmospheric pressure pulses recorded on microbarographs. M.Sc. thesis, Department of Physics, Colorado School of Mines, Golden, Colorado.

Spillane, K.T. and McCarthy, M.J., 1969. Downdraft of the organized thunderstorm. Aust. Met. Mag., 17, 3-24.

Stokes, G.G., 1880. Mathematical and physical papers, 1, 197, Cambridge University Press.

Wallington, C.E., 1961. Observations of the effects of precipitation downdraughts. Weather, 16, 35-43.

Welch, P.D., 1967. The use of fast Fourier transforms for the estimation of power spectra; a method based on time averaging over short modified periodograms. Trans. IEEE AU-15, 2, 70-73.

ACKNOWLEDGEMENTS

The authors wish to express their gratitude to Dr. J.F. Gettrust for several helpful discussions during the course of this research and for the use of an efficient filter routine. In addition, they wish to thank Sgt. Chadwick and other members of the United States Air Force for assistance in the installation of the infrasonic array and Mr. David Daffen and Mr. Blair Lade for their efforts in operating and maintaining the Warramunga Seismic Station.

TABLE 1: Internal Solitary Waves

Event Number	Day	Time (U.T.)	Apparent Velocity c (m/sec)	Azimuth (degrees)	Signal Amplitude a ($dynes/cm^2$)	Full Width at Half Maximum $W_{1/2}$ (km)
			1975			
1-2-976	238	1216	4	340	150	0.14
1-2-1207	238	2020	8	20	590	0.19
1-4-223	240	1324	4	240	40	0.48
1-4-846	241	1012	4	120	40	0.19
1-4-1797	242	1756	10	40	90	0.75
1-4-2524	243	1807	7	210	100	0.73
2-1-343	244	1730	14	20	80	1.68
2-1-982	245	1448	12	150	300	0.86
3-1-956	254	1416	10	280	160	1.40
3-2-1846	260	1018	4	20	40	0.24
3-2-2110	260	1906	8	60	260	0.28
3-2-2717	261	1520	13	140	70	1.21
4-1-1242	263	1852	10	40	610	0.39
4-1-1965	264	1856	10	20	300	0.65
4-2-312	265	1632	12	140	190	1.21
4-2-862	266	1050	10	140	50	0.70
4-4-767	270	1825	10	30	90	1.06
4-4-1321	271	2151	10	240	310	0.98
5-3-512	276	2038	10	230	300	2.68
5-4-990	279	1802	9	20	50	1.56
6-1-1054	282	1548	10	330	80	0.28
6-1-2350	284	1055	14	180	450	1.20
6-3-1797	290	1254	9	200	100	0.64
7-2-188	291	0834	12	20	530	0.79
7-2-338	291	1232	16	340	170	1.93
7-2-1601	293	0737	10	220	430	1.10
7-2-1623	293	0822	16	300	700	1.79
7-3-1050	297	1258	4	100	60	0.21
7-3-1110	297	1458	12	140	80	0.68
7-3-1238	297	1914	11	140	100	1.18
7-3-3304	300	1614	12	140	100	0.39

Event Number	Day	Time (U.T.)	Apparent Velocity c (m/sec)	Azimuth (degrees)	Signal Amplitude a (dynes/cm^2)	Full Width at Half Maximum $w_{\frac{1}{2}}$ (km)
8-1-433	301	1600	11	20	70	1.06
8-1-1699	303	2108	6	160	60	0.47
8-1-1716	303	2144	10	240	190	1.30
8-2-1081	307	1518	6	0	40	0.36
8-2-1180	307	1822	6	120	80	0.47
9-3-618	316	2042	10	100	50	0.60
9-3-1132	317	1350	6	80	40	1.01
9-3-1242	317	1728	8	80	530	0.26
9-4-442	318	1742	6	40	300	0.25
10-3-1074	325	1414	10	20	60	0.75
10-3-1205	325	1836	8	20	70	0.72
10-4-518	327	1750	9	20	100	0.73
10-5-973	329	1500	8	140	80	0.95
10-6-472	330	1726	12	160	80	0.43
11-1-534	331	1810	8	160	140	1.38
11-2-996	334	1012	8	160	90	0.72
11-3-1046	337	1300	8	20	80	0.56
11-4-406	339	1426	10	60	190	0.80
12-3-352	345	1330	7	140	50	1.15
12-4-1108	347	1350	7	120	90	0.70
13-2-192	351	1222	14	320	160	1.36
13-2-334	351	1702	8	20	130	2.40
13-4-408	357	1506	10	120	70	0.50
13-4-1744	359	1140	6	160	70	0.34
13-4-1833	359	1436	9	40	140	1.40
13-4-2573	360	1516	8	40	180	0.86
14-1-462	361	1510	8	160	90	0.45
14-1-1146	362	1400	10	20	160	1.02
14-1-1902	363	1510	8	20	250	0.60
			1976			
17-2-1763	29	1409	8	160	40	0.72
18-1-224	51	1354	8	160	70	0.96
18-2-1292	55	2238	12	120	70	0.82

Event Number	Day	Time (U.T.)	Apparent Velocity c (m/sec)	Azimuth (degrees)	Signal Amplitude a (dynes/cm^2)	Full Width at Half Maximum $W_{1/2}$ (km)
18-3-404	56	1336	9	40	180	1.02
18-3-1099	57	1234	9	0	240	0.76
18-4-529	58	1906	7	60	100	0.95
19-1-536	60	1750	11	140	50	2.06
19-2-1972	68	1822	8	140	150	0.36
19-2-2036	68	2032	8	20	330	0.61
20-1-418	70	1418	12	140	240	1.14
20-1-1883	72	1506	14	20	120	1.81
20-2-286	73	1083	8	20	260	0.81
20-3-918	77	1106	16	0	70	1.60
21-3-1960	85	1908	9	100	40	1.17
22-1-315	87	1708	10	60	30	0.90
22-1-1115	88	1950	12	120	40	1.32
22-2-1812	91	1710	10	120	50	0.52
22-2-1918	91	2046	14	80	90	0.81
22-2-2517	92	1636	11	140	50	1.01
24-2-1826	107	1318	8	100	70	0.81
24-2-2067	107	2118	6	100	50	0.90
31-1-1111	158	1346	10	140	70	0.45
31-1-1133	158	1435	12	140	150	0.71
33-2-963	178	1016	5	140	30	0.30
33-2-997	178	1124	4	180	30	0.21

FIGURE CAPTIONS

1. Configuration of the five-component microbarograph array.

2. Measured microbarograph amplitude response.

3. Internal solitary wave surface pressure profiles corresponding to a $5^{o}K$ temperature inversion at the 950 mbar level. The dimensionless amplitude, α, is chosen to be 0.5.

   (a) Classical internal solitary wave described by (3.5)

   (b) Internal solitary wave described by Benjamin's theory (3.8) for a fluid of great depth.

4. General internal solitary wave profile shape as a function of the dimensionless amplitude α. Both families of curves are plotted in the dimensionless quantities X/H and Y/H where H is the undisturbed depth of the lower fluid at infinity.

   (a) Shallow fluid theory

   (b) Deep fluid theory.

5. Examples of solitary wave spectra recorded at the Warramunga Seismic Station. These well-defined waves of elevation are typical of most of the large amplitude events which have been observed.

6. Further examples of solitary waves of elevation. Note the sudden change in the character of the micropressure spectrum following the passage of the solitary wave illustrated in (a).

7. Various forms of solitary wave spectra. Figure (a) in this group is chosen to illustrate an example of a solitary wave of elevation followed by a solitary wave of depression.

8. Examples of solitary waves of elevation which preceed a decaying train of coherent long period spectral components.

9. Examples of solitary waves of elevation which mark the onset of long period incoherent components in the atmospheric spectrum.

10. Examples of microbarograph records which illustrate a variety of unusual solitary wave profiles.

11. Frequency of observation of solitary wave signals as a function of calendar day.

12. Frequency of observation of solitary waves as a function of time of day.

13. Occurrence of solitary waves as a function of source azimuth.

14. Diurnal variation of the micropressure spectrum illustrating the growth and dissipation of the nocturnal inversion and the influence of solitary wave activity.

15. Some examples of the influence of solitary waves on the atmospheric spectrum.

16. A comparison of solitary wave pressure profiles for the case of (a) a wave with a relatively quiet wake, and (b) a wave which preceeds a period of significant atmospheric turbulence.

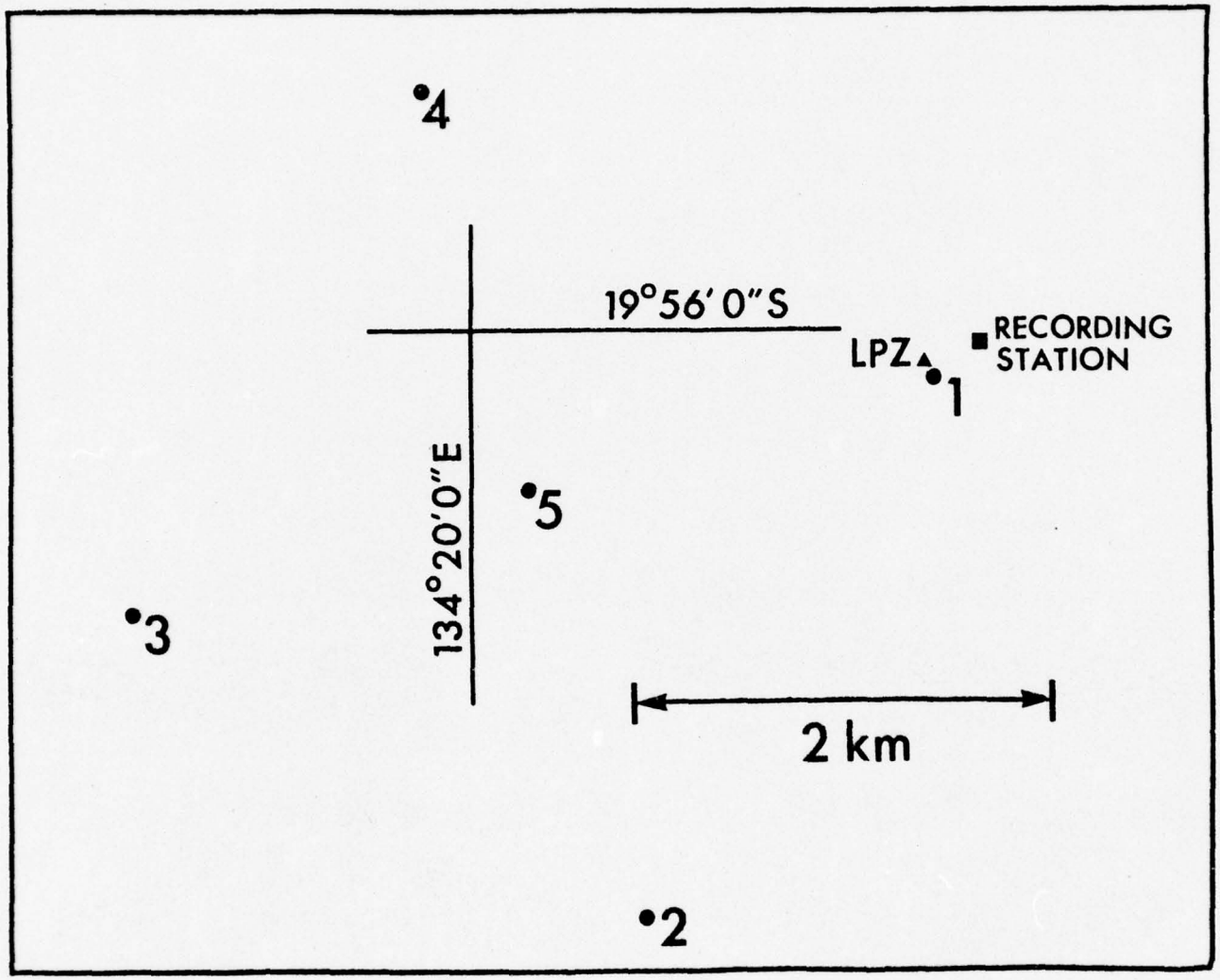

Figure 1.

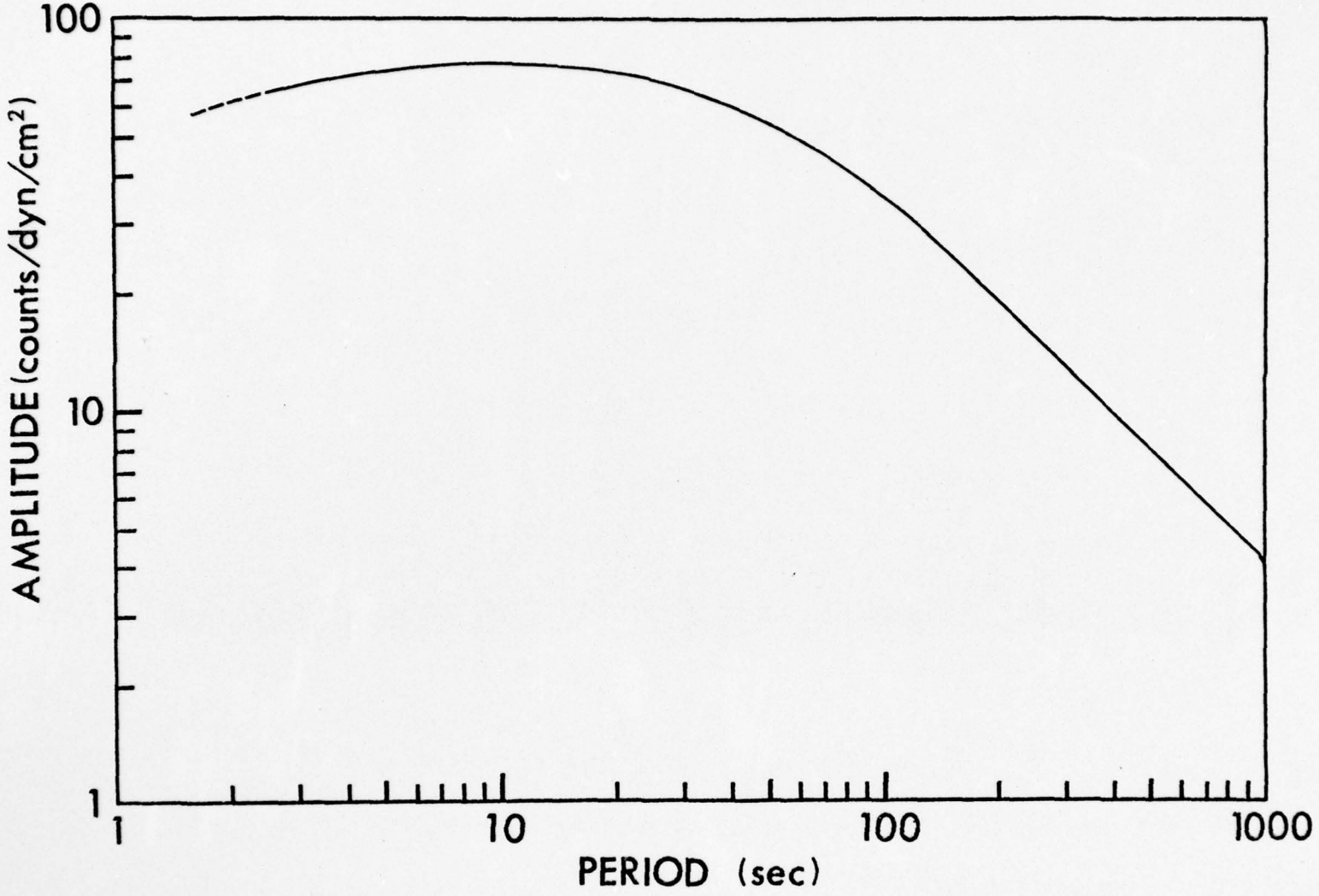

Figure 2.

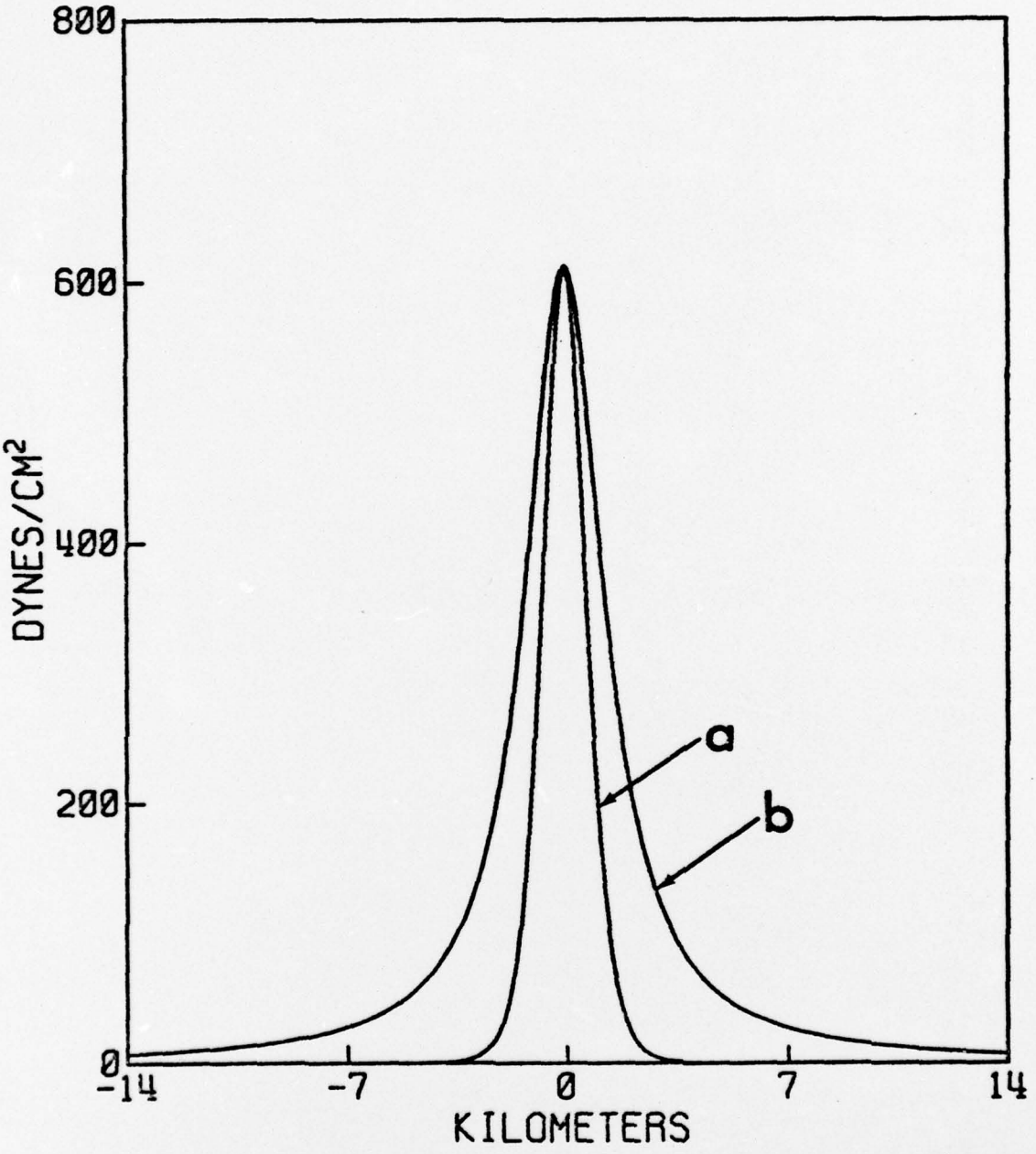

Figure 3.

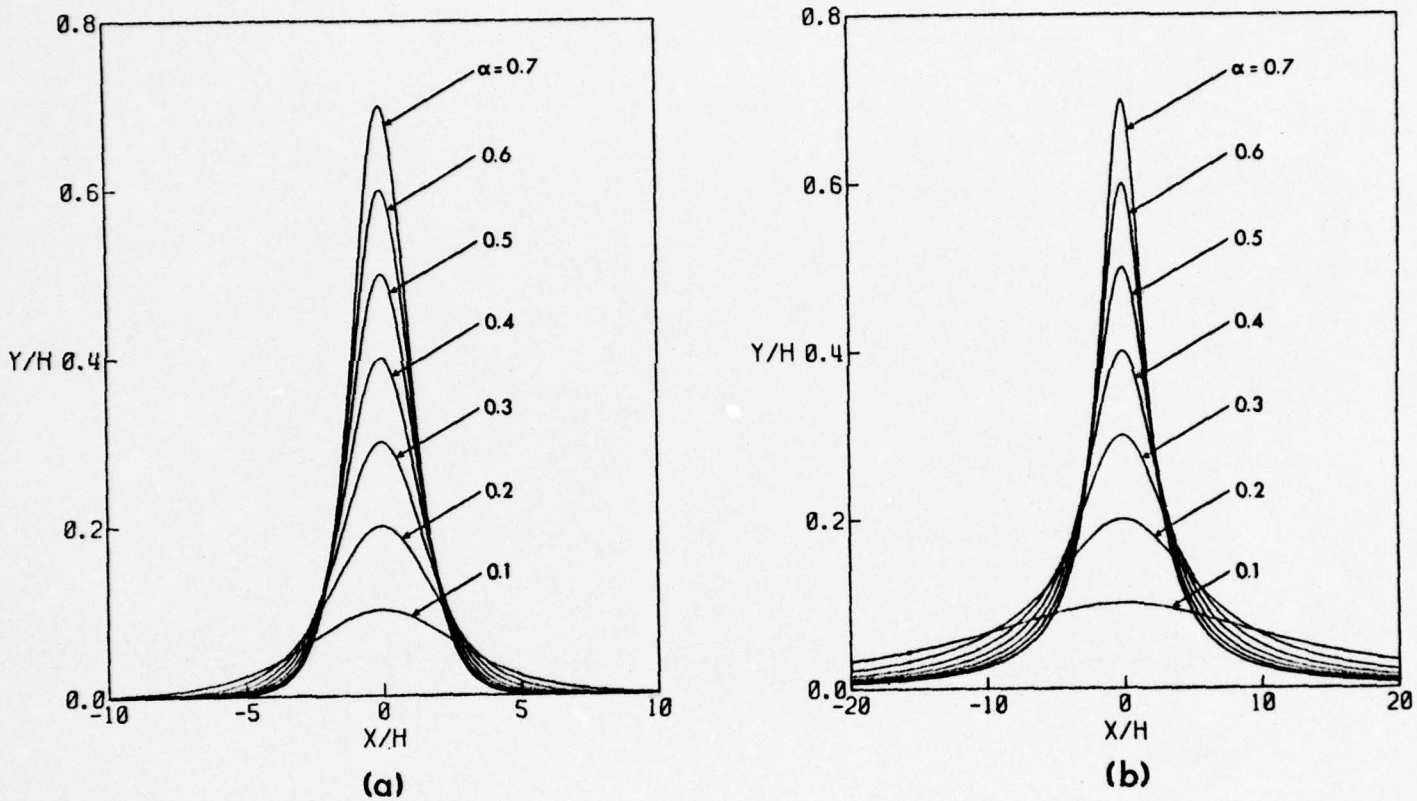

Figure 4.

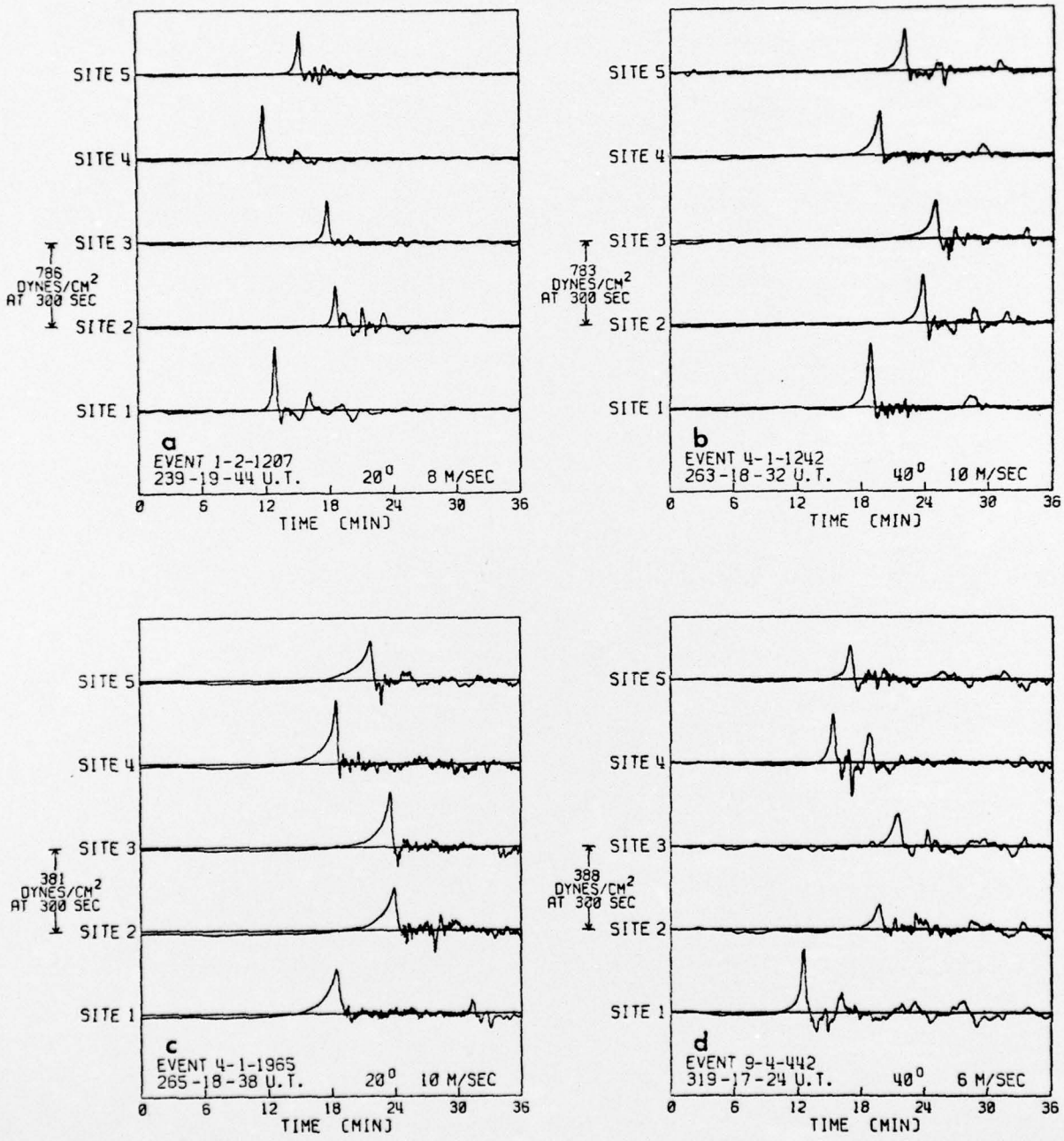
SITE 5
SITE 4
SITE 3
SITE 2
SITE 1
786 DYNES/CM² AT 300 SEC
a
EVENT 1-2-1207
239-19-44 U.T.
20° 8 M/SEC
0 6 12 18 24 30 36
TIME (MIN)
783 DYNES/CM² AT 300 SEC
b
EVENT 4-1-1242
263-18-32 U.T.
40° 10 M/SEC
381 DYNES/CM² AT 300 SEC
c
EVENT 4-1-1965
265-18-38 U.T.
20° 10 M/SEC
388 DYNES/CM² AT 300 SEC
d
EVENT 9-4-442
319-17-24 U.T.
40° 6 M/SEC

Figure 5.

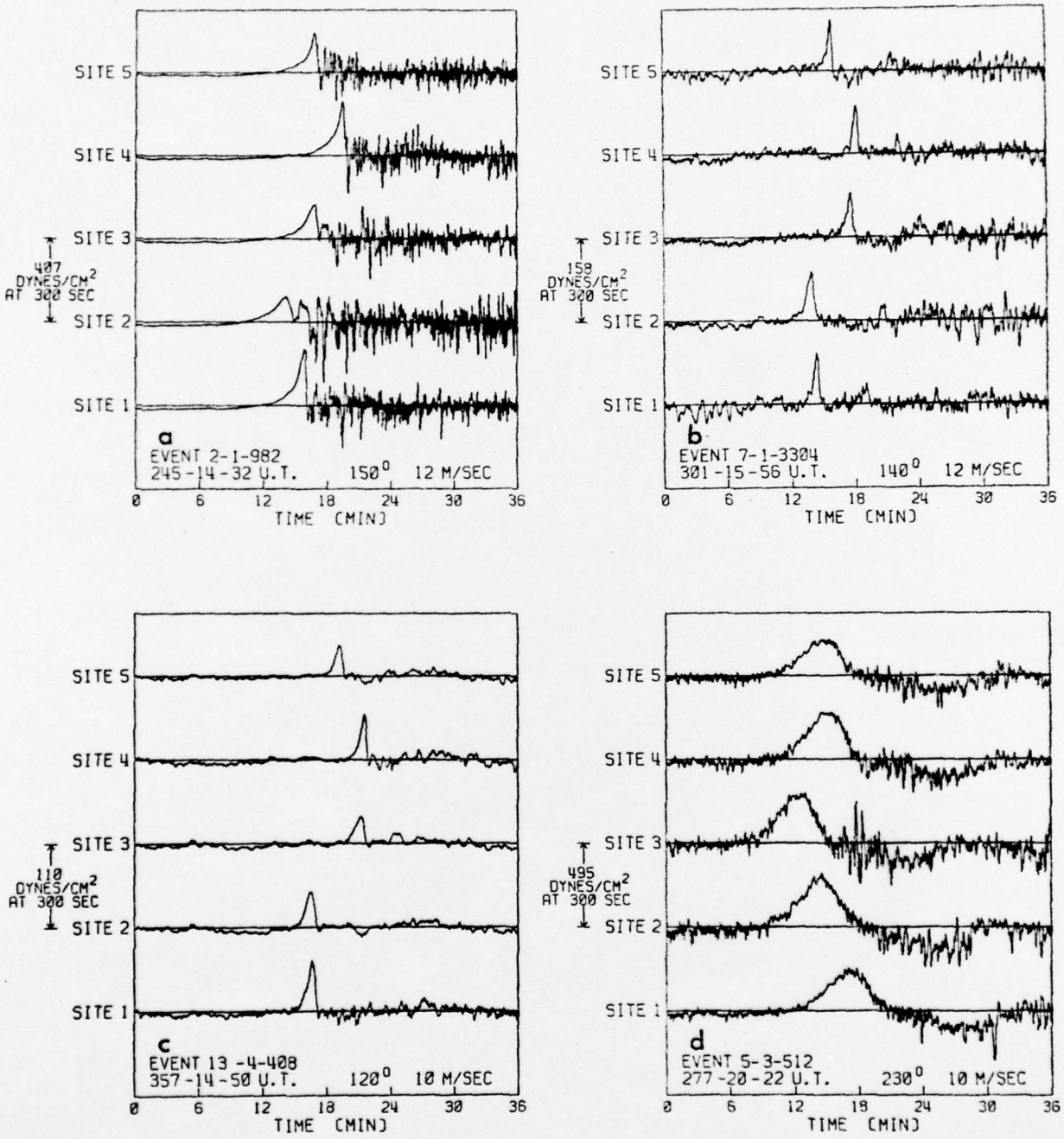
SITE 5
SITE 4
SITE 3
SITE 2
SITE 1
407 DYNES/CM² AT 300 SEC
a
EVENT 2-1-982
245-14-32 U.T.
150° 12 M/SEC
0 6 12 18 24 30 36
TIME (MIN)
158 DYNES/CM² AT 300 SEC
b
EVENT 7-1-3304
301-15-56 U.T.
140° 12 M/SEC
110 DYNES/CM² AT 300 SEC
c
EVENT 13-4-408
357-14-50 U.T.
120° 10 M/SEC
495 DYNES/CM² AT 300 SEC
d
EVENT 5-3-512
277-20-22 U.T.
230° 10 M/SEC

Figure 6.

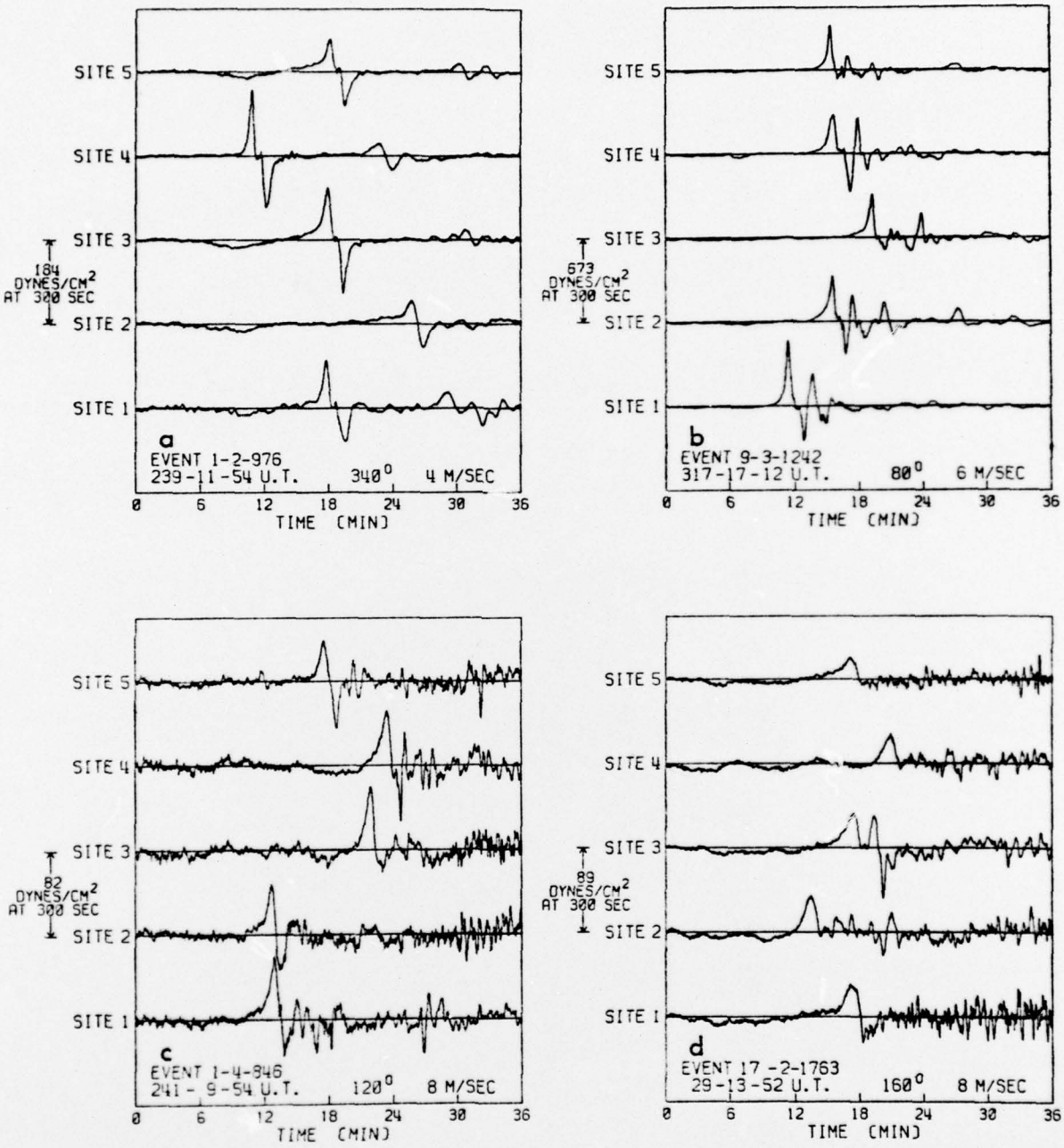
SITE 5
SITE 4
SITE 3
SITE 2
SITE 1
184 DYNES/CM² AT 300 SEC
a
EVENT 1-2-976
239-11-54 U.T.
340°
4 M/SEC
673 DYNES/CM² AT 300 SEC
b
EVENT 9-3-1242
317-17-12 U.T.
80°
6 M/SEC
82 DYNES/CM² AT 300 SEC
c
EVENT 1-4-846
241-9-54 U.T.
120°
8 M/SEC
89 DYNES/CM² AT 300 SEC
d
EVENT 17-2-1763
29-13-52 U.T.
160°
8 M/SEC
0 6 12 18 24 30 36
TIME (MIN)

Figure 7.

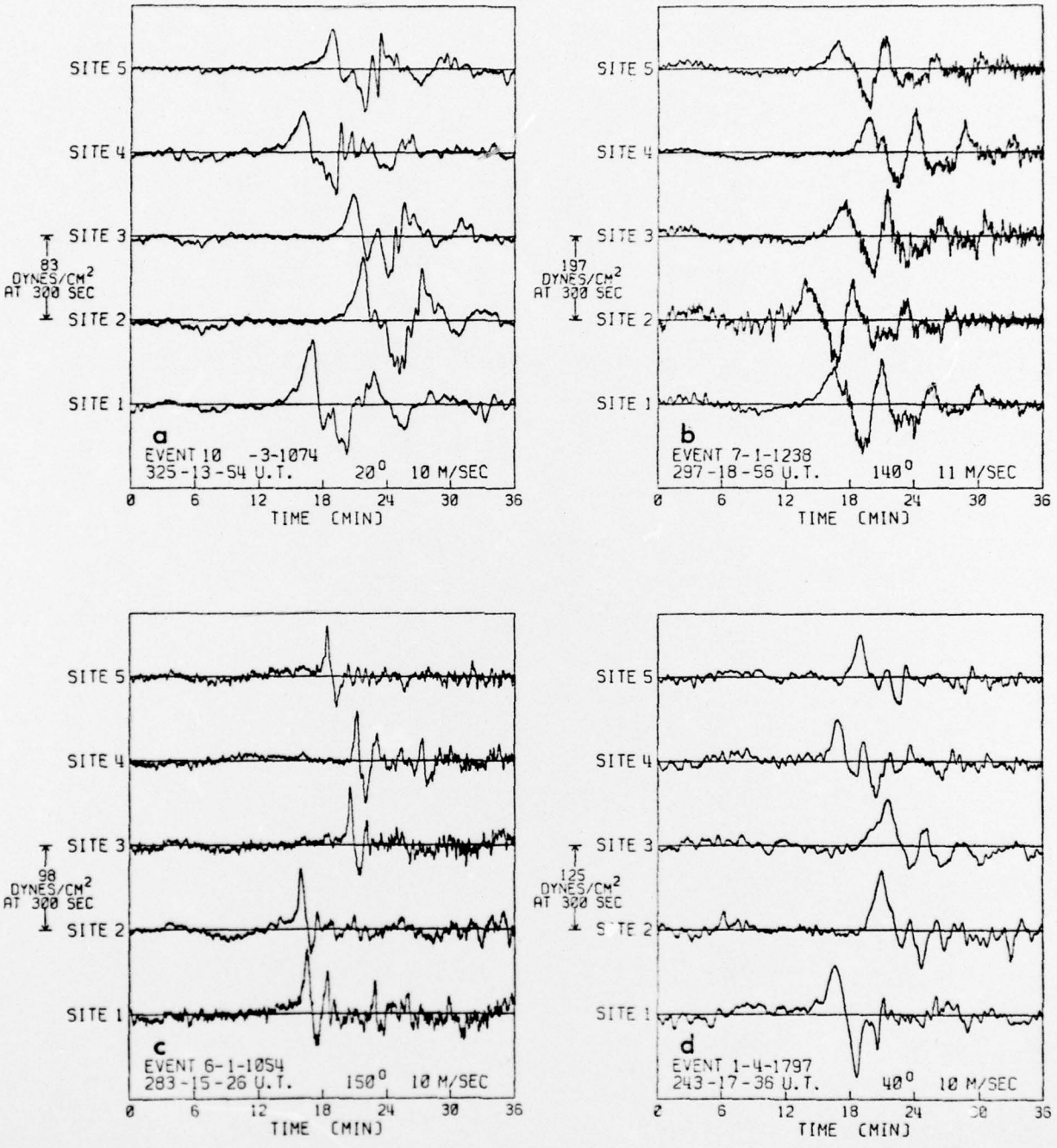
SITE 5
SITE 4
SITE 3
SITE 2
SITE 1
83 DYNES/CM² AT 300 SEC
a
EVENT 10 -3-1074
325-13-54 U.T.
20°
10 M/SEC
0 6 12 18 24 30 36
TIME (MIN)
197 DYNES/CM² AT 300 SEC
b
EVENT 7-1-1238
297-18-56 U.T.
140°
11 M/SEC
98 DYNES/CM² AT 300 SEC
c
EVENT 6-1-1054
283-15-26 U.T.
150°
10 M/SEC
125 DYNES/CM² AT 300 SEC
d
EVENT 1-4-1797
243-17-36 U.T.
40°
10 M/SEC

Figure 8.

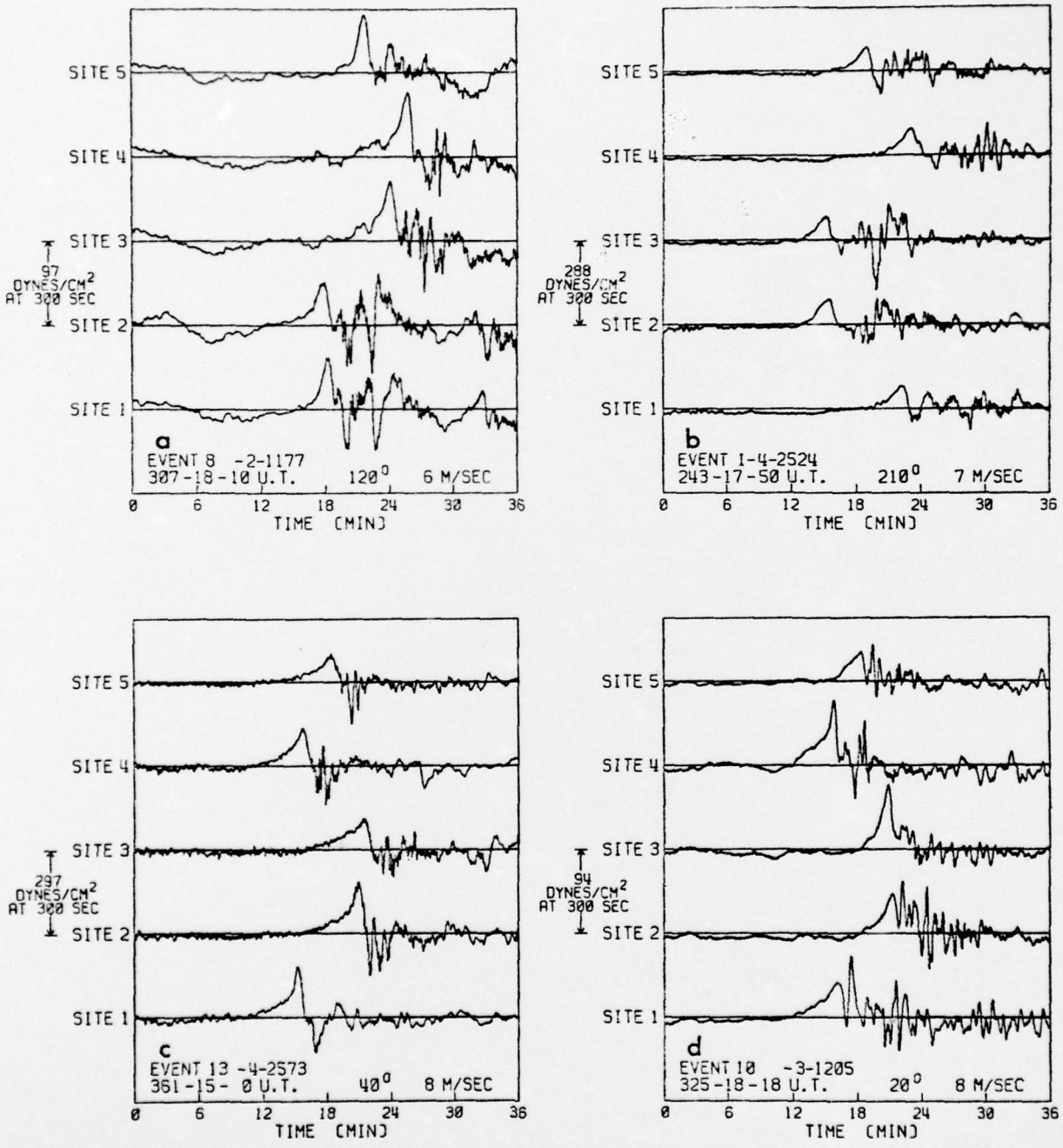
SITE 5
SITE 4
SITE 3
SITE 2
SITE 1
97 DYNES/CM² AT 300 SEC
a
EVENT 8 -2-1177
307-18-10 U.T. 120° 6 M/SEC
0 6 12 18 24 30 36
TIME (MIN)
288 DYNES/CM² AT 300 SEC
b
EVENT 1-4-2524
243-17-50 U.T. 210° 7 M/SEC
297 DYNES/CM² AT 300 SEC
c
EVENT 13 -4-2573
361-15- 0 U.T. 40° 8 M/SEC
94 DYNES/CM² AT 300 SEC
d
EVENT 10 -3-1205
325-18-18 U.T. 20° 8 M/SEC

Figure 9.

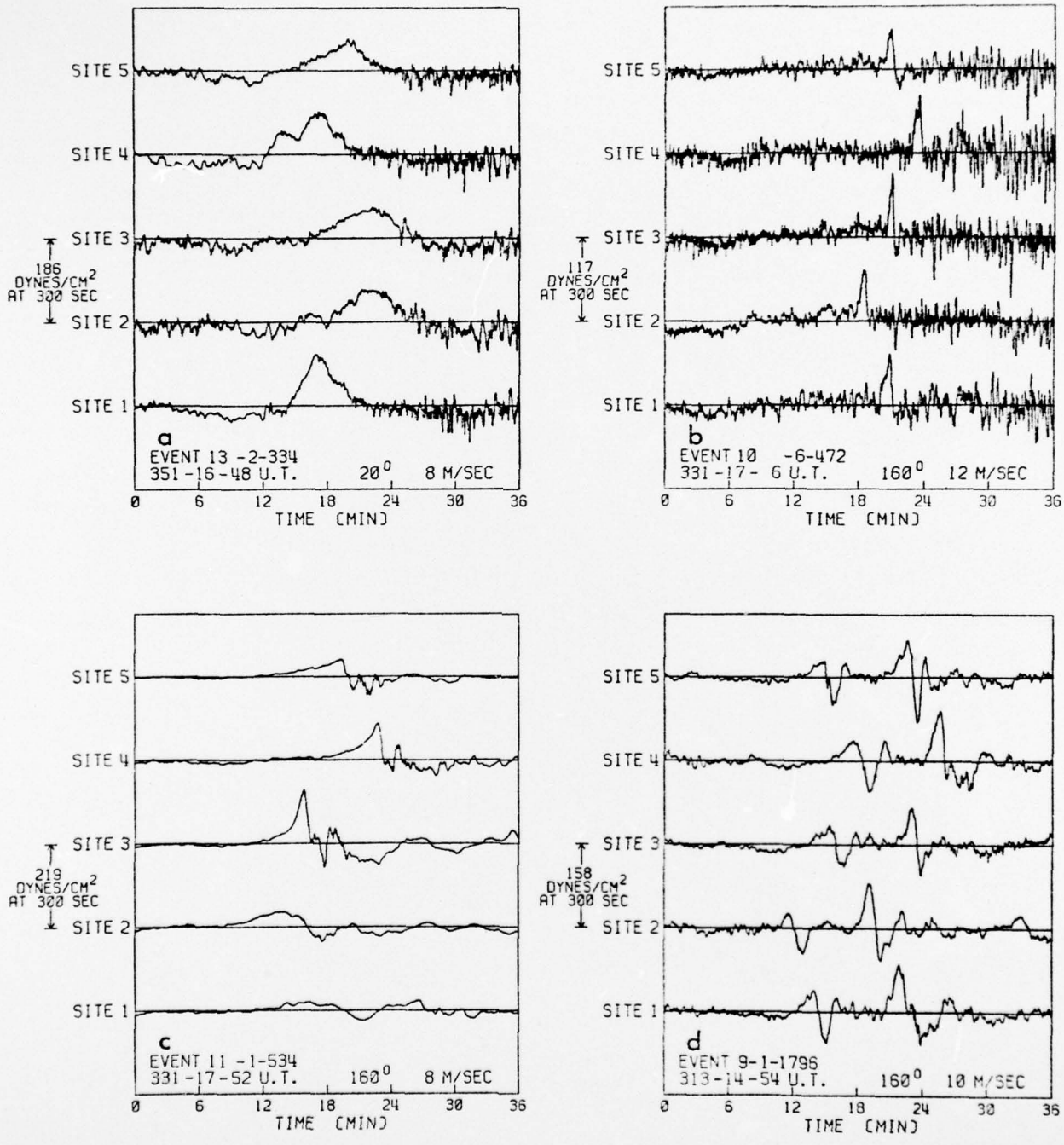
SITE 5
SITE 4
SITE 3
SITE 2
SITE 1
186 DYNES/CM² AT 300 SEC
a
EVENT 13 -2-334
351-16-48 U.T.
20°
8 M/SEC
0 6 12 18 24 30 36
TIME (MIN)
117 DYNES/CM² AT 300 SEC
b
EVENT 10 -6-472
331-17- 6 U.T.
160°
12 M/SEC
219 DYNES/CM² AT 300 SEC
c
EVENT 11 -1-534
331-17-52 U.T.
160°
8 M/SEC
158 DYNES/CM² AT 300 SEC
d
EVENT 9-1-1796
313-14-54 U.T.
160°
10 M/SEC

Figure 10.

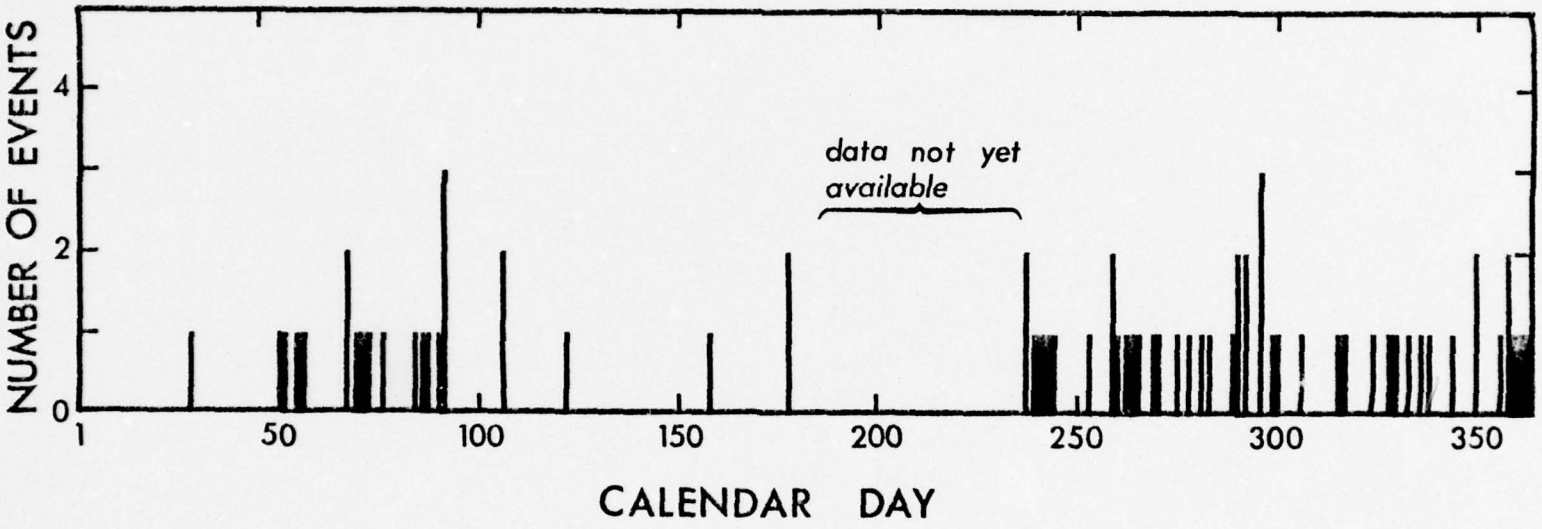
NUMBER OF EVENTS
0
2
4
data not yet
available
1
50
100
150
200
250
300
350
CALENDAR DAY

Figure 11.

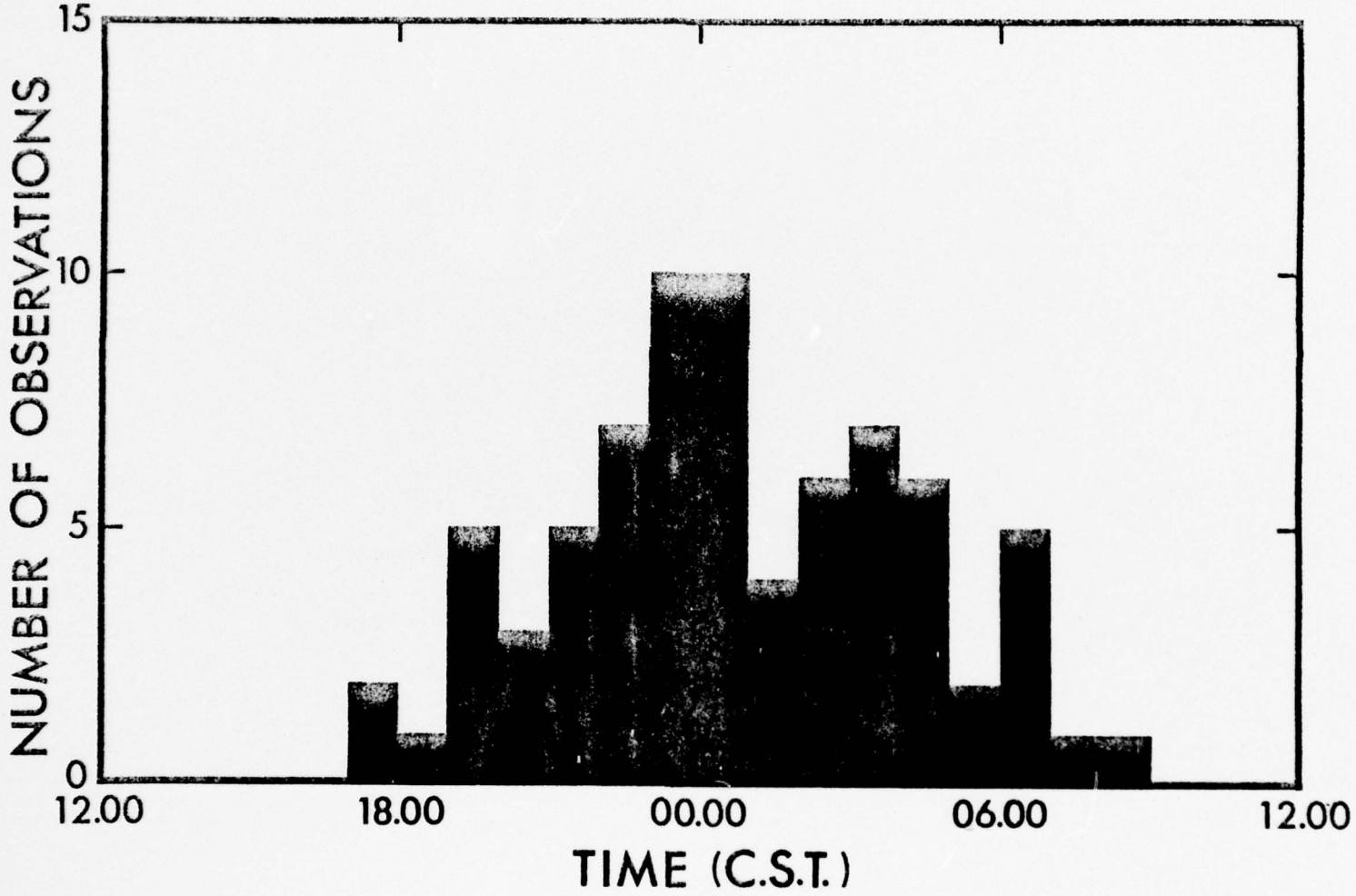
15
10
5
0
NUMBER OF OBSERVATIONS
12.00
18.00
00.00
06.00
12.00
TIME (C.S.T.)

Figure 12.

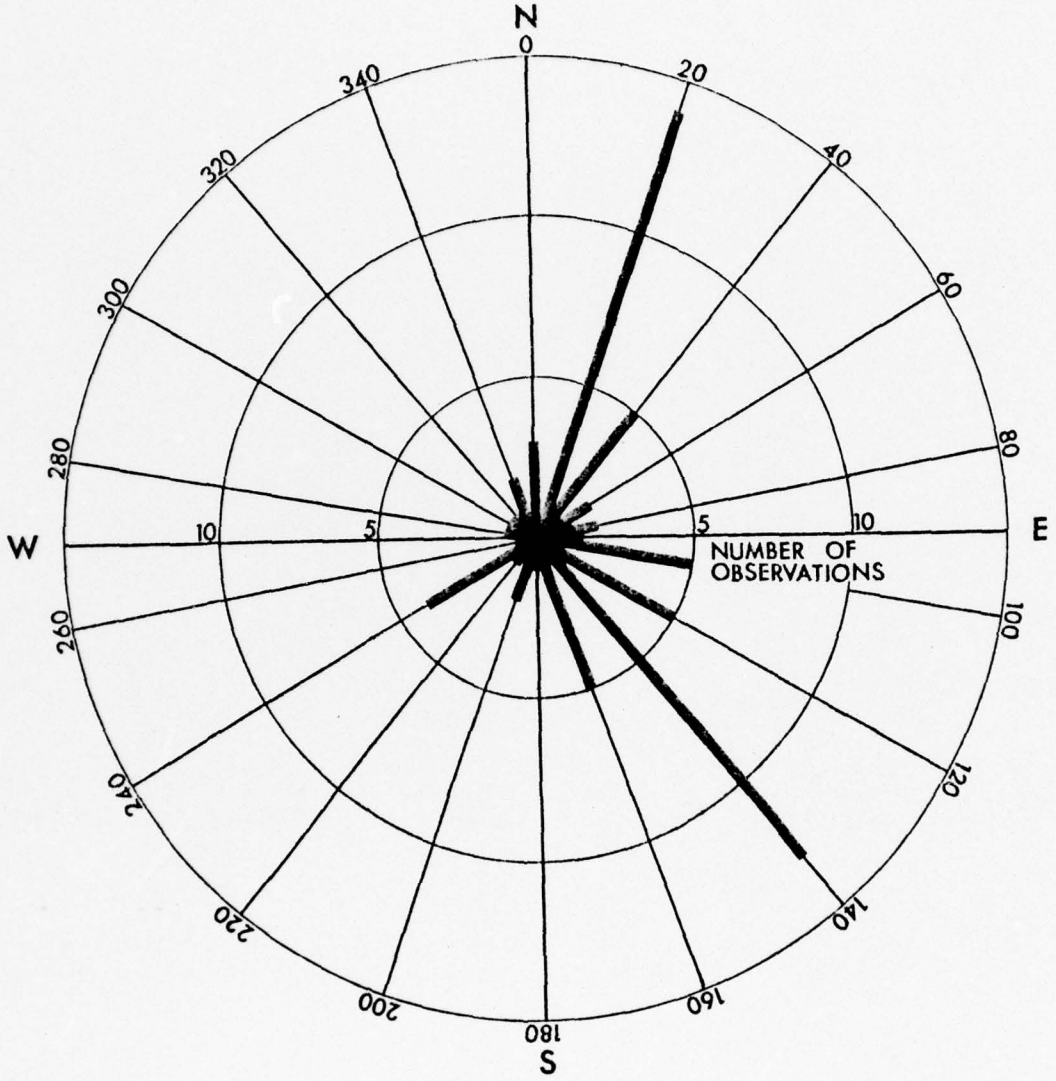
N
0
20
40
60
80
E
100
120
140
160
180
S
200
220
240
260
280
W
300
320
340
10
5
5
10
NUMBER OF
OBSERVATIONS

Figure 13.

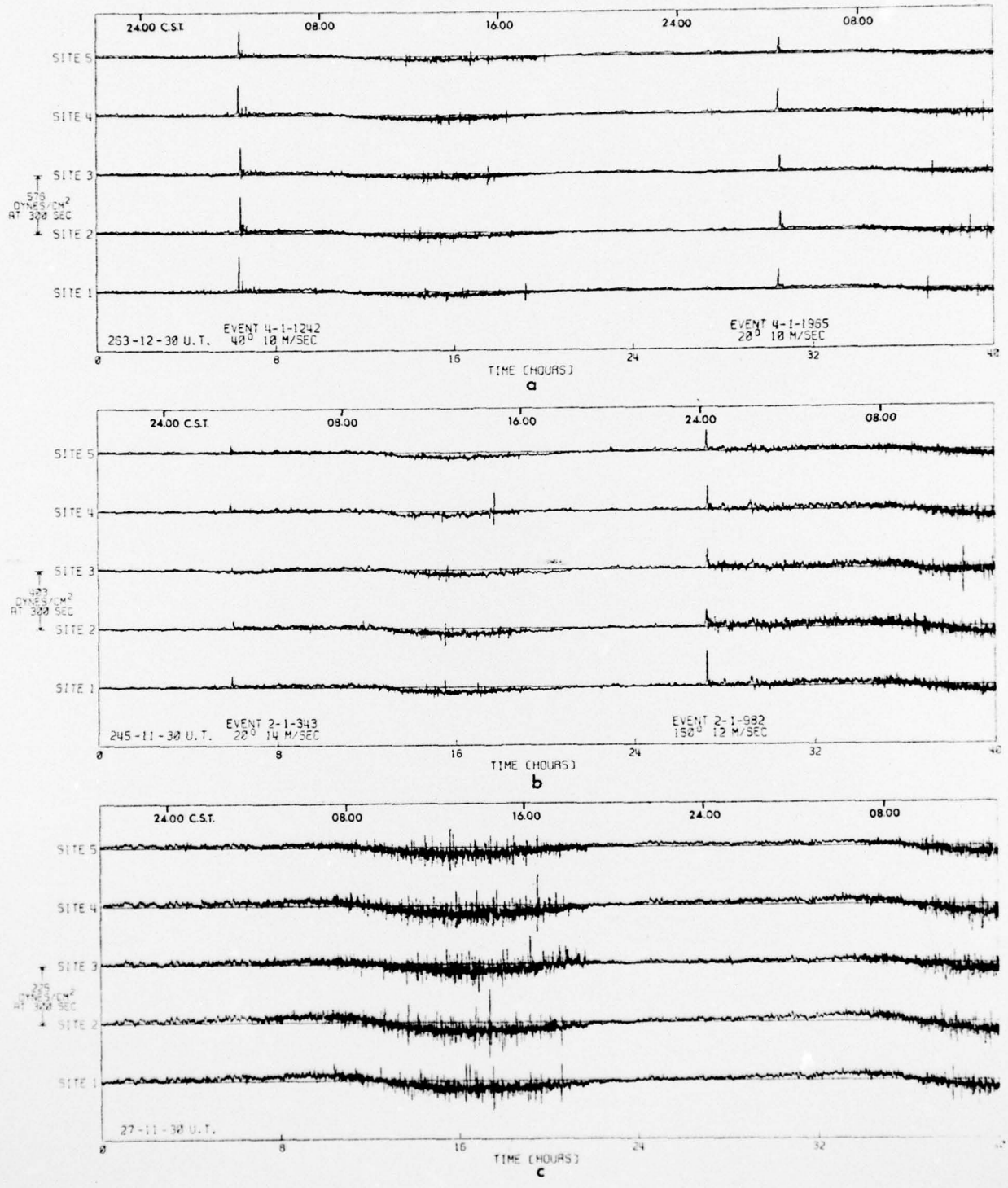
24.00 C.S.T.
08.00
16.00
24.00
08.00
SITE 5
SITE 4
SITE 3
SITE 2
SITE 1
579 DYNES/CM² AT 300 SEC
263-12-30 U.T.
EVENT 4-1-1242
40° 10 M/SEC
EVENT 4-1-1965
20° 10 M/SEC
0
8
16
24
32
40
TIME (HOURS)
a
24.00 C.S.T.
08.00
16.00
24.00
08.00
SITE 5
SITE 4
SITE 3
SITE 2
SITE 1
422 DYNES/CM² AT 300 SEC
245-11-30 U.T.
EVENT 2-1-343
22° 14 M/SEC
EVENT 2-1-992
150° 12 M/SEC
0
8
16
24
32
40
TIME (HOURS)
b
24.00 C.S.T.
08.00
16.00
24.00
08.00
SITE 5
SITE 4
SITE 3
SITE 2
SITE 1
225 DYNES/CM² AT 300 SEC
27-11-30 U.T.
0
8
16
24
32
TIME (HOURS)
c

Figure 14.

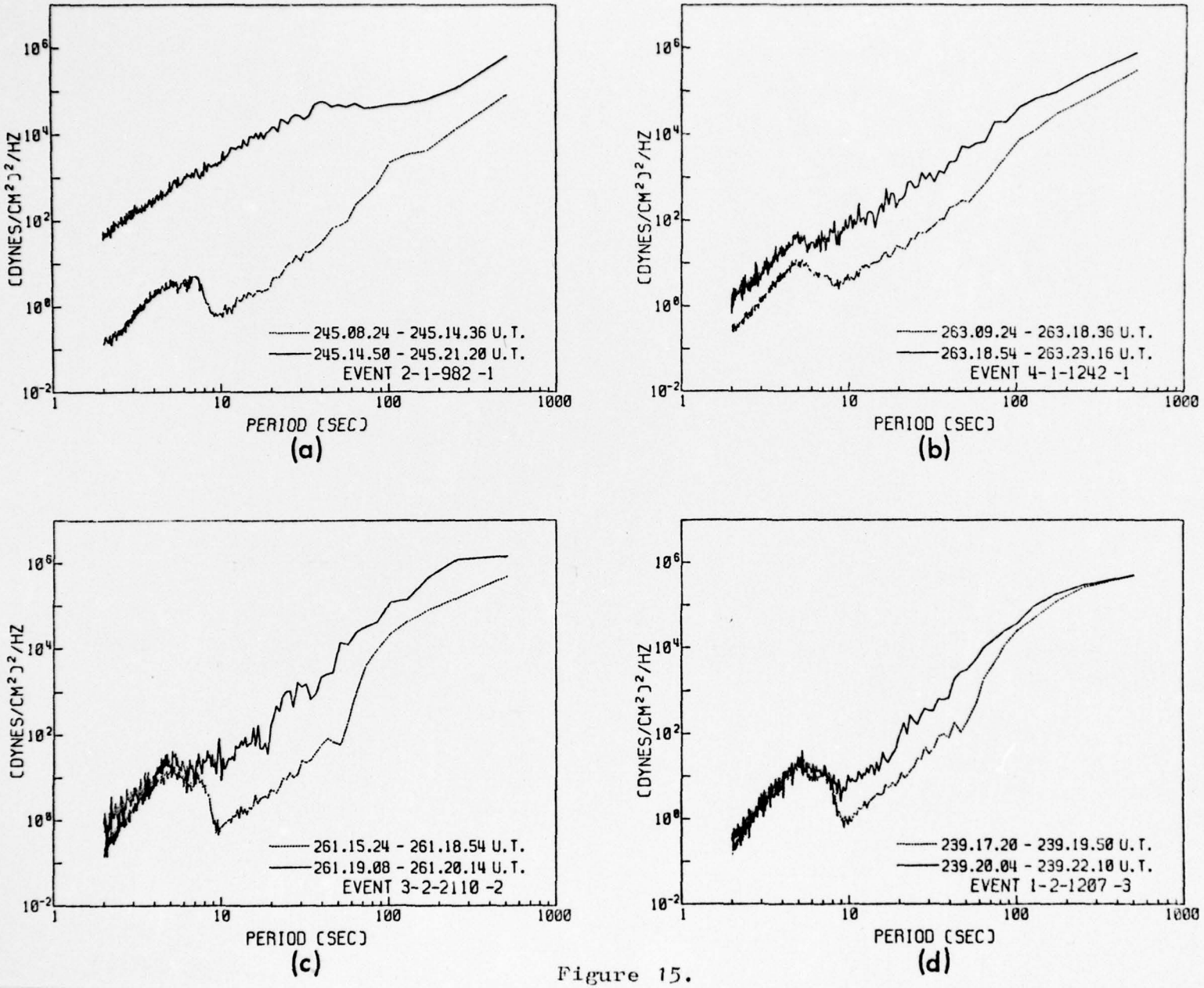
(DYNES/CM²)²/HZ
PERIOD (SEC)
245.08.24 - 245.14.36 U.T.
245.14.50 - 245.21.20 U.T.
EVENT 2-1-982 -1
(a)
263.09.24 - 263.18.36 U.T.
263.18.54 - 263.23.16 U.T.
EVENT 4-1-1242 -1
(b)
261.15.24 - 261.18.54 U.T.
261.19.08 - 261.20.14 U.T.
EVENT 3-2-2110 -2
(c)
239.17.20 - 239.19.50 U.T.
239.20.04 - 239.22.10 U.T.
EVENT 1-2-1207 -3
(d)

Figure 15.

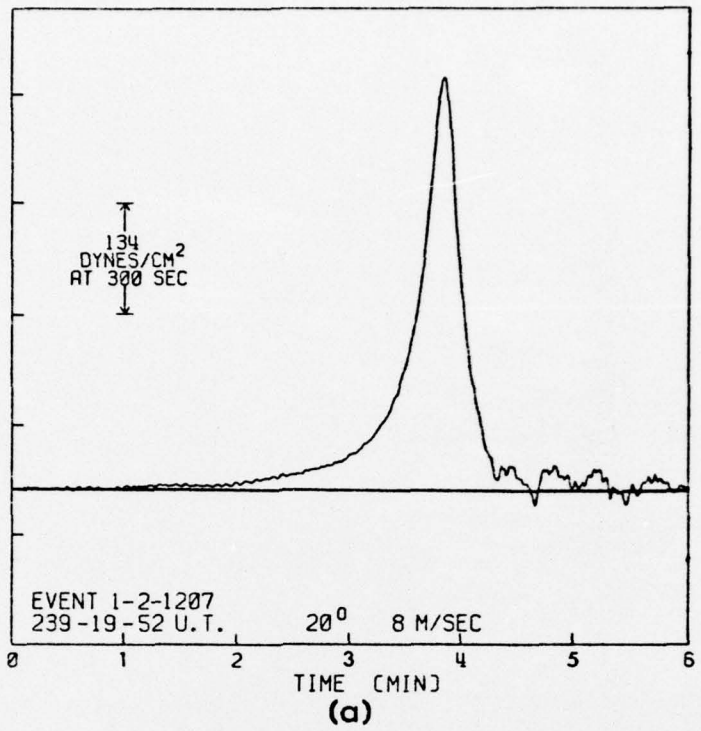
134
DYNES/CM2
AT 300 SEC
EVENT 1-2-1207
239-19-52 U.T.
20°
8 M/SEC
0
1
2
3
4
5
6
TIME (MIN)

(a)

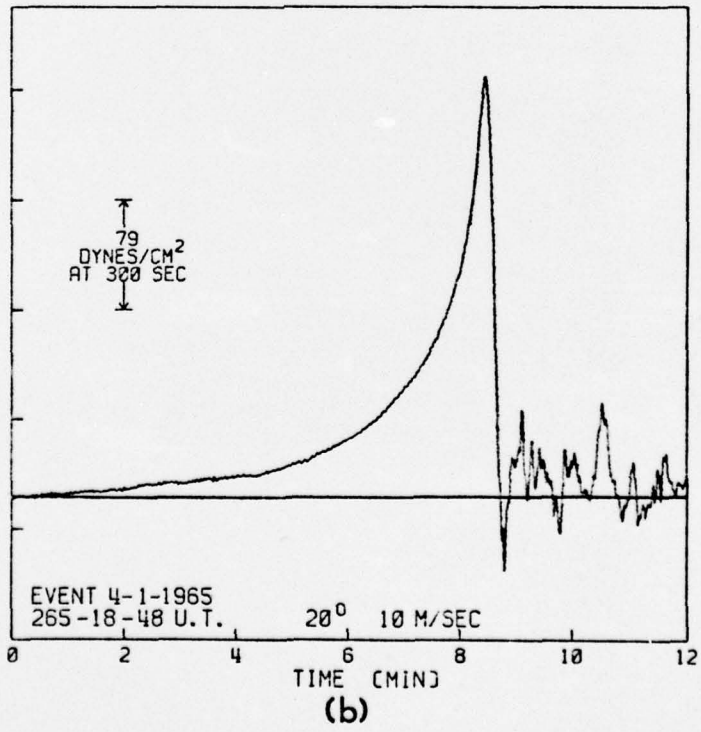
79
DYNES/CM2
AT 300 SEC
EVENT 4-1-1965
265-18-48 U.T.
20°
10 M/SEC
0
2
4
6
8
10
12
TIME (MIN)

(b)

Figure 16.